In Vivo Melanoma Cell Morphology Reflects Molecular Signature and Tumor Aggressiveness

Journal:	*Journal of Investigative Dermatology*
Manuscript ID	JID-2021-0439
Article Type:	Original Article
Date Submitted by the Author:	19-May-2021

Complete List of Authors:	Marconi, Alessandra; University of Modena and Reggio Emilia, Surgical, Medical, Dental and Morphological Science Quadri, Marika; University of Modena and Reggio Emilia, Laboratory of Cutaneous Biology, Department of Surgical, Medical, Dental and Morphological Sciences Farnetani, Francesca; University of Modena and Reggio Emilia, Dermatology Unit, Department of Surgical, Medical, Dental and Morphological Sciences with Interest in Transplant, Oncological and Regenerative Medicine Ciardo, Silvana; University of Modena and Reggio Emilia, Dermatology Unit, Department of Surgical, Medical, Dental and Morphological Sciences with Interest in Transplant, Oncological and Regenerative Medicine PALAZZO, ELISABETTA; University of Modena and Reggio Emilia, Laboratory of Cutaneous Biology, Department of Surgical, Medical, Dental and Morphological Sciences Lotti, Roberta; University of Modena and Reggio Emilia, Laboratory of Cutaneous Biology, Department of Surgical, Medical, Dental and Morphological Sciences Cesinaro, Anna ; Azienda Ospedaliero-Universitaria di Modena Policlinico di Modena, Department of Pathology Fabbiani, Luca; University of Modena and Reggio Emilia, Department of medical and surgical sciences Vaschieri, Cristina ; University of Modena and Reggio Emilia, DermoLAB, Department of Surgical, Medical, Dental and Morphological Science Puviani, Mario; Sassuolo Hospital, Unit of Dermatology and Surgical Dermatology Magnoni, Cristina; University of Modena and Reggio Emilia, Dermatology Unit; Surgical, Medical and Dental Department of Morphological Sciences related to Transplant, Oncology and Regenerative Medicine Kaleci, Shaniko; Universita degli Studi di Modena e Reggio Emilia, Dermatology Unit, Department of Surgical, Medical, Dental and Morphological Science with Interest Transplant, Oncological and Regenerative Medicine Pincelli, Carlo; University of Modena and Reggio Emilia, Laboratory of Cutaneous Biology, Department of Surgical, Medical, Dental and Morphological Sciences Pellacani, Giovanni; University of Modena and Reggio Emilia, Dermatology; University of Rome La Sapienza, Dermatology Clinic, Department of Clinical Internal, Anesthesiology and Cardiovascular

1
2
3
4
5
6
7
8
9
10
11
12
13
14
15
16
17
18
19
20
21
22
23
24
25
26
27
28
29
30
31
32
33
34
35
36
37
38
39
40
41
42
43
44
45
46
47
48
49
50
51
52
53
54
55
56
57
58
59
60

	Sciences
Keywords:	Melanoma, Imaging, Microscopy, Cancer Biology, Gene Transcription

SCHOLARONE™
Manuscripts

1
2
3
4
5
6
7
8
9
10
11
12
13
14
15
16
17
18
19
20
21
22
23
24
25
26
27
28
29
30
31
32
33
34
35
36
37
38
39
40
41
42
43
44
45
46
47
48
49
50
51
52
53
54
55
56
57
58
59
60

In Vivo Melanoma Cell Morphology Reflects Molecular Signature and Tumor Aggressiveness

Alessandra Marconi[1]* (ORCID: 0000-0002-5667-5766), Marika Quadri[1]* (ORCID: 0000-0001-7619-660X), Francesca Farnetani[2] (ORCID: 0000-0001-7088-9077), Silvana Ciardo[2] (ORCID: 0000-0002-2381-2189), Elisabetta Palazzo[1] (ORCID: 0000-0002-0812-5524), Roberta Lotti[1] (ORCID: 000-0003-2126-4147), Anna Maria Cesinaro[3] (ORCID: 0000-0001-6807-8152), Luca Fabbiani[4] (0000-0002-0104-5249), Cristina Vaschieri[1] (ORCID: 0000-0001-6434-2681), Mario Puviani[5] (ORCID: 0000-0003-1792-2581), Cristina Magnoni[2] (0000-0002-6081-4925), Shaniko Kaleci[2] (0000-0002-1166-2961), Carlo Pincelli[1] (ORCID: 0000-0003-4416-2637) and Giovanni Pellacani[2,6] (ORCID: 0000-0002-7222-2951)

[1] DermoLAB, Department of Surgical, Medical, Dental and Morphological Science, University of Modena and Reggio Emilia, Modena, Italy

[2] Dermatology Unit, Department of Surgical, Medical, Dental and Morphological Sciences, University of Modena and Reggio Emilia, Modena, Italy

[3] Department of Pathology, Azienda Ospedaliero-Universitaria Policlinico, Modena, Italy.

[4] Department of Medical and Surgical Sciences, University of Modena and Reggio Emilia, Modena, Italy

[5] Unit of Dermatology and Surgical Dermatology, Sassuolo Hospital, Sassuolo, Modena, Italy.

[6] Dermatology Clinic, Department of Clinical Internal, Anesthesiology and Cardiovascular Sciences, La Sapienza University of Rome, Italy

* The authors contributed equally to this work

For Review Only

Corresponding author: Alessandra Marconi, DermoLAB, Department of Surgical, Medical, Dental and Morphological Science, University of Modena and Reggio Emilia, via Del Pozzo 71, 41124, Modena, Italy; Tel.: +39 059 4222812; Fax: +39 059 4224271; Mail: alessandra.marconi@unimore.it

Short Title: Bio-molecular characterization of RCM-melanoma subtypes

Abbreviations: Reflectance Confocal Microscopy (RCM), Dendritic cell melanoma (DC) Round Cell melanoma (RC), Dermal Nest melanoma (DN), Combined type melanoma (CT).

For Review Only

ABSTRACT

Melanoma is the deadliest type of skin cancer, characterized by high cellular heterogeneity which contributes to therapy resistance and unpredictable disease outcome. Recently, by correlating Reflectance-Confocal-Microscopy (RCM) morphology with histopathological type, we identified four distinct melanoma-subtypes: dendritic-cell (DC), round-cell (RC), dermal-nest (DN), and combined-type (CT) melanomas. In the present study, each RCM melanoma-subtype expressed a specific biomolecular profile and biological behavior *in vitro*. Markers of tumor aggressiveness, including Ki67, MERTK, nestin and stemness markers, were highest in the most invasive CT and DN melanomas, as compared to DC and RC. This was also confirmed in multicellular tumor spheroids. Transcriptomic analysis showed a modulation of cancer-progression-associated genes from DC to CT melanomas. The switch from E- to N-cadherin expression proved the epithelial-to-mesenchymal transition from DC to CT subtypes. The DN melanoma was predominantly located in the dermis, as also shown in skin reconstructs. It displayed a unique behavior and a molecular profile associated with a high degree of aggressiveness. Altogether, our results demonstrate that each RCM-melanoma subtype has a distinct biological and gene expression profile, related to tumor aggressiveness, confirming that

1
2
3
4
5
6
7
8
9
10
11
12
13
14
15
16
17
18
19
20
21
22
23
24
25
26
27
28
29
30
31
32
33
34
35
36
37
38
39
40
41
42
43
44
45
46
47
48
49
50
51
52
53
54
55
56
57
58
59
60

RCM can be a dependable tool for *in vivo* detecting different types of melanoma and for early diagnostic screening.

Introduction

Melanoma is an extremely aggressive skin cancer consisting of several cell populations that show diverse genotypic and phenotypic features, signalling pathway, biological behaviour, and response to therapy, suggesting the existence of a heterogeneous family of diseases rather than a unique entity (Scolyer et al., 2011). Melanoma is characterized by high metastatic capacity, resistance to conventional chemotherapy and in part to new targeted drugs (Rodriguez-Cerdeira et al., 2017). Given its threatening potential, early detection remains the key factor in lowering melanoma-associated mortality. Classification is important for tumor diagnosis and prognosis. Melanoma is currently classified based on different parameters such as histopathological type, vertical growth, spreading to nearby lymph nodes or any other organs (Arrangoiz et al., 2016). However, it has become clear that this classification and staging system fail to account for different progression models of melanoma and to pre-select patients for a specific treatment (Broekaert et al., 2010). This implies the need for new criteria and methodology to classify melanoma.

Reflectance-confocal-microscopy (RCM) is an emerging technology for the non-invasive analysis of skin tissue in real-time and at near-histopathological resolution (Fink and Haenssle, 2016). Recently, we proposed the existence of four distinct melanoma-subtypes based on the correlation between RCM-observed cell-morphology and histopathological/patients' clinical features: 1) Dendritic-Cell (DC) with a predominant population of dendritic-cells in the epidermal layer; 2) Round-Cell (RC) mostly composed of large roundish-cell population in the epidermal layer and dermal-epidermal junction (DEJ); 3) Dermal-Nest (DN) characterized by the presence of a dermal cerebriform nesting in the dermis; 4) Combined-Type (CT) which shows a

For Review Only

1 2 3 4 5 6 7 8 9 10 11 12 13 14 15 16 17 18 19 20 21 22 23 24 25 26 27 28 29 30 31 32 33 34 35 36 37 38 39 40 41 42 43 44 45 46 47 48 49 50 51 52 53 54 55 56 57 58 59 60

combination of all three confocal patterns (Pellacani et al., 2014). Previous work showed a correlation between patients' features and melanoma-subtypes, suggesting that RCM cell-morphology may be associated with different tumor stage and biological behavior (Graziottin et al., 2016). Accordingly, a biological heterogeneity among RCM-subtypes based on the different expression of tumor-associated biomarkers was recently shown (Beretti et al., 2018). It is known that specific genetic alterations are associated with precise clinical and histopathological features of melanoma, indicating that they may be helpful in refining existing disease classification (Whiteman et al., 2011). Yet, the existence of a close correlation between RCM-melanoma subtypes, genetic signature and biological behavior remains to be clarified.

In this work, we detected significant modifications in the expression of specific melanoma biomarkers in the RCM-subtypes and we present evidence that the four melanoma-groups display different genetic profile and biological behaviour *in vitro*, which closely correlate with tumor aggressiveness.

For Review Only

Results

RCM-subtypes reflect patient/tumor characteristics.

90 patients, with a median age of 60.9 years, were analysed in this study (Table 1). Representative clinical, histopathological and RCM images are illustrated in Figure 1a-f. DC melanomas were mainly of the RGP type (92%), with a Breslow index (BI) of less than 1mm and a mitotic index (MI) between 0 and 1 (both 96%). Moreover, DC presented significantly less $BRAF^{V600E}$ mutations than the other RCM subtypes. An increase in tumor thickness (BI) was found in RC melanomas, as compared to DC. RC were either of the RGP or VGP type (56% and 44% respectively), despite their low MI (96% between 0-1). On the other hand, CT and DN were mostly of the VGP type (96% and 93% respectively), showing high MI (40% 2-5mm). DN melanomas were significantly thicker than the other RCM-types (5.8mm). 36% of

patients with DC type had a previous history of melanoma and 40% of them relapsed or developed new melanomas, as compared to the other RCM subtypes. However, none of DC types progressed to metastases. On the contrary, CT and DN significantly tended to metastasize, as revealed by the percentage of positive sentinel lymph nodes (32 and 27% respectively) and metastases at 0-5 years (20 and 34 %, respectively).

RCM-morphology correlates with aggressiveness, stemness markers expression and biological behavior *in vitro.*

To analyze the growth fraction in each RCM-subtype, the expression of Ki67 proliferation-marker was evaluated both in the epidermis and dermis (Figure 2a). DC melanomas showed the expression of Ki67 exclusively in the epidermis, whereas DN melanomas showed it in the dermis. By comparing DC and RC melanomas, the expression of Ki67 in RC was mainly localized in the epidermis with fraction of positive cells in the dermis, suggesting its more aggressive behavior compared to DC melanoma. Conversely, CT expressed elevated levels of Ki67 both in epidermis and dermis.

C-MER proto-oncogene tyrosine kinases (MERTK) and the intermediate filament Nestin are associated with melanoma aggressiveness and progression (Schlegel et al., 2013; Klein et al., 2007). The expression of these markers significantly raised from DC to CT/DN melanomas, while no differences were observed between CT and DN (Figure 2a).

The expression of Hypoxia transcription factor (HIF) 1α, which is known to stimulate angiogenesis (Widmer et al., 2013), was significantly higher in RC, as compared to the other RCM-subtypes. Moreover, the expression of SOX-10, known to affect melanoma cell proliferation, survival, and invasion (Graf et al., 2014), significantly increased from DC to CT-DN melanomas (Figure 2a).

1
2
3
4
5
6
7
8
9
10
11
12
13
14
15
16
17
18
19
20
21
22
23
24
25
26
27
28
29
30
31
32
33
34
35
36
37
38
39
40
41
42
43
44
45
46
47
48
49
50
51
52
53
54
55
56
57
58
59
60

The melanoma-initiating-cells (MICs), significantly contributing to initiation, metastasis, and recurrence of melanoma, consist of a cell subpopulation expressing various markers such as the ABC-transporter-5 (ABCB5) (Chartrain et al., 2012), CD133 (Monzani et al., 2007), SOX-2 (Santini et al, 2014) and CD271 (Boiko et al., 2010). ABCB5 expression significantly increased from DC to CT-DN melanomas, whereas no differences were found between CT and DN. On the contrary, SOX-2 and CD133 were significantly more expressed in DN. CD271 expression considerably increased from DC to RC, while it decreased from RC to CT/DN melanomas. The latter finding is not unexpected given the controversial role of CD271 in melanoma. Despite it is considered a MICs marker, CD271 downregulation has been shown to promote melanoma progression and invasion (Saltari et al., 2016) (Figure 2b).

To define the biological behaviour of RCM-subtypes, freshly-isolated cells from melanoma biopsies were seeded as Multicellular-Tumor-Spheroids (MCTSs) (Figure 2c). While CT and DN cells were able to generate spheroids, DC and RC failed to form compact MCTSs , probably due to their less proliferative capacity (Figure 2d). Consistently, CT and DN showed a greater proliferative ability than DC and RC (Figure 2e). Altogether, these data suggest that CT and DN contain the most aggressive tumor cell populations, given their major expression of aggressiveness-associated markers and their higher proliferative capacity *in vitro*. Notably, DN showed higher expression levels of the MIC's markers CD133 and SOX-2, as compared the other RCM-subtypes, indicating the peculiarity of this melanoma subtype.

RCM-subtypes display different gene expression profiles.

To characterize the RCM-subtypes at the molecular level, a transcriptome analysis associated with cancer-progression was performed. Using DAVID Functional-Association-Tool, we analyzed the differentially expressed genes among groups and a Biological Process (BP) enrichment was obtained for each RCM-subtypes (Figure 3a). In detail, we observed a

For Review Only

1 2 3 4 5 6 7 8 9 10 11 12 13 14 15 16 17 18 19 20 21 22 23 24 25 26 27 28 29 30 31 32 33 34 35 36 37 38 39 40 41 42 43 44 45 46 47 48 49 50 51 52 53 54 55 56 57 58 59 60

progressive increase in extracellular-matrix (ECM) remodeling, angiogenesis, and inflammation BP terms from DC to CT melanomas. Conversely, a downregulation of the genes involved in cell-adhesion was found from DC to CT. On the other hand, DN gene expression profile appeared to deviate from the other RCM-subtypes, showing a distinct pattern of gene expression associated with ECM-remodeling, angiogenesis, inflammation, and cell-adhesion. Moreover, a modulation of cancer-associated transcription factor (TF) gene expression among the different groups was identified. SMAD and BMP signaling pathways, stem cell differentiation, bicellular-tight-junction assembly and positive regulation of cell differentiation BPs where the most significantly modulated TF-associated-genes. This is consistent with the functional role of those genes in tumor progression (Schlegel et al., 2013; Caramel et al., 2013; Rusciano, 2000).

We further evaluated the gene expression profile of the RCM-subtypes as compared to the less aggressive DC type (Figure 3b-c). By uploading each comparison into Venny 2.1, we identified 55 (25.6%) and 60 genes (27.97%) that were specifically upregulated in RC and CT vs DC, respectively, while only 16 genes (7.4%) were upregulated in DN vs DC. Conversely, 128 genes (68.5%) were downregulated in DN vs DC, while only 7 (2.7%) and 18 (6.8%) genes were downregulated in RC vs DC and CT vs DC, respectively. Subsequently, for each comparison, we analyzed the specific pathways belonging to the unique or common gene profile, by uploading the corresponding gene list on PANTHER Classification-System (Figure S1-S2, Figure 3b-c). Slight differences in gene modulation were found in RC vs DC. Up and down-regulated genes in this comparison were mainly involved in the first steps of inflammation (mediated by chemokine/cytokines), regulation of cytoskeleton and cadherin signaling pathway. A modulation of genes involved in integrin and cadherin signaling pathway and angiogenesis were found in CT vs DC, suggesting an increase of tumor aggressiveness in CT compared to DC/RC. Moreover, we found a variation in genes involved in the advanced steps

For Review Only

1
2
3 of inflammation (B and T-cell activation), and angiogenesis in DN vs DC melanomas,
4
5 suggesting that DN could be a highly aggressive tumor. Survivin is considered a biomarker of
6
7
8 poor prognosis in melanoma (Takeuchi et al., 2005), and the expression of CXCL8 positively
9
10 correlates with tumor progression (Ugurel et al., 2001), while CD271 downregulation has been
11
12 associated to melanoma progression and invasion (Saltari et al., 2016). The expression of
13
14
15 *BIRC5* (Survivin), and *CXCL8* mRNA significantly raised from DC to CT-DN melanomas,
16
17 suggesting a progressive increase in tumor aggressiveness. On the other hand, *NGFR* mRNA
18
19 (CD271) increased from DC to RC and subsequently decreased from RC to CT/DN in a
20
21
22 statistically significative manner, confirming the immunohistochemical results (Figure 3d).
23
24
25
26 **RCM-morphology reflects tumor aggressiveness and progression stage.**
27
28
29 The above results indicate that RC subtypes show intermediate characteristics between DC and
30
31 CT melanomas. To further confirm this finding, we analysed the most significant pathways in
32
33 RC vs DC and CT vs RC subtypes (Figure S3; Figure 4a-b). As expected, only few genes were
34
35
36 significantly modulated in RC vs DC melanomas (Figure 4a). In detail, TGF-β and WNT-
37
38 Signaling pathway associated genes were found to be upregulated in RC, as compared to DC
39
40 melanomas. Consistently, TGF-β isoforms promote tumor invasiveness *in vitro* (Javelaud et
41
42
43 al., 2008), while WNT-signaling plays an important role in the crosstalk between key oncogenic
44
45 pathways involved in melanoma development and progression (Gajos-Michniewicz and
46
47 Malgorzata, 2020). The interactions between chemokine and their receptors can independently
48
49
50 protect against tumor development and growth or they can stimulate melanoma tumor
51
52 progression and metastasis (Richmond et al., 2009). In our context, both up and downregulation
53
54 of genes involved in this type of inflammation were found. Moreover, the upregulation of
55
56
57 *CXCL8* in RC melanomas confirmed their more aggressive behavior, as compared to DC.
58
59 By comparing CT and RC melanomas, we found a substantial gene modulation related to
60

For Review Only

1
2
3
4
5
6
7
8
9
10
11
12
13
14
15
16
17
18
19
20
21
22
23
24
25
26
27
28
29
30
31
32
33
34
35
36
37
38
39
40
41
42
43
44
45
46
47
48
49
50
51
52
53
54
55
56
57
58
59
60

integrins and cadherins signaling pathways (Figure S3; Figure 4b). During melanoma progression, a modulation of cell-adhesion molecules is known to guide the phenotype switching that promote cell migration (Haass et al., 2005). High levels of β1 and β3-integrin are known to promote melanoma transition from RPG to VPG type (Ramakrishnan et al., 2006), while αvβ3 and αvβ5-integrins are involved in angiogenesis, being upregulated on endothelial cells during tumor neovascularization (Eskens et al., 2003). Moreover, the T-cadherin downregulation (*CDH13* gene) was found to influence migration and invasion (Bosserhoff et al., 2013). Genes related to β3-integrin and to angiogenesis were upregulated while CDH13 was downregulated in CT melanomas (Figure S4; Figure 3b), highlighting its more aggressive behavior, as compared to RC.

Recently, we have shown that CD271 downregulation plays a role in promoting melanoma progression and invasion, at least in part because of the lack of cell-cell-adhesion molecule (Saltari et al., 2016). CD271 expression increased from DC to RC and, subsequently, turned off from RC to CT (Figure 2b and Figure 3d). In RCM-subtypes with different thickness, CD271 expression directly correlated with BI in the less aggressive RCM subtypes, while it inversely correlated in more advanced tumors (BI >1 mm) (Figure 4c). At the same time, we found that the E-cadherin expression significantly decreased from DC to CT, suggesting a progressive loss of epithelial cell-adhesion molecules, which was paralleled by an increase of N-cadherin from CT to DC melanomas (Figure 4e).

CT and DN subtypes show a different gene expression profile and biological behavior *in vitro*.

Data reported here suggest that CT and DN are the most aggressive tumors, and DN reveals a unique gene expression profile. To evaluate the difference between these two types of tumors, the up and downregulated genes in CT vs DN were analysed by PANTHER and then clustered

For Review Only

1
2
3
4
5
6
7
8
9
10
11
12
13
14
15
16
17
18
19
20
21
22
23
24
25
26
27
28
29
30
31
32
33
34
35
36
37
38
39
40
41
42
43
44
45
46
47
48
49
50
51
52
53
54
55
56
57
58
59
60

according to the most significant pathways involved (Figure S4; Figure 5a). Several genes were up and downregulated in CT vs DN, highlighting the differences between these tumor types. To further investigate the difference between CT and DN, their function was analysed *in vitro* by using 3D-models (Figure S5; Figure 5b). The *in vitro* invasion assay revealed that DN melanomas were significantly more invasive than CT (Figure 5c-d). Moreover, DN cells reached a longer distance from spheroid, as compared to CT cells (Figure 5f). In melanoma skin reconstructs, CT cells were observed at the DEJ. Contrariwise, DN cells were able to growth only when seeded directly into the dermis, (Figure 5g), displaying a high proliferative capacity, as shown by the % of Ki67 positive cells (Figure 5h). E-cadherin was scarcely detected in DN melanoma, which expressed elevated levels of N-cadherin, as compared to CT. The higher expression of α4 and α7-integrin in DN compared to CT confirmed the greater invasive behavior of this tumor. Additionally, DN expressed significantly increased levels of SOX-2 compared to CT, confirming its more undifferentiated state (Figure 5h). Moreover, while invading cells from DN-spheroids expressed higher level of α4-integrin, confirming the aggressiveness of this tumor type, CD271 was scarcely detectable in these cells (Figure 5i).

Discussion

Melanoma progression depends on diverse phases where the stepwise acquisition of genetic abnormalities contributes to the increase of aggressiveness (Thompson et al., 2005). Distinguishing between these stages may be important to have a more accurate diagnosis and prognosis. It has been shown that RCM-subtypes might reflect specific clinical patterns. DC is mainly associated to a slow-intra-epidermal growing tumor, mainly characterized by single cell vs. nest proliferation, while RC shows a predominantly horizontal pattern of growth with a tendency to form nests and to infiltrate the dermis. Conversely, DN shows a rapid pattern of growth with higher BI (Pellacani et al., 2014). Consistently, our study demonstrates a

For Review Only

1
2
3
4
5
6
7
8
9
10
11
12
13
14
15
16
17
18
19
20
21
22
23
24
25
26
27
28
29
30
31
32
33
34
35
36
37
38
39
40
41
42
43
44
45
46
47
48
49
50
51
52
53
54
55
56
57
58
59
60

progressive increase of the clinical pattern severity going from DC to CT-DN melanomas. Moreover, DC develop more melanomas in time or relapses than the other RCM-subtypes, suggesting an association with a prolonged sun exposure. Conversely, CT and DN metastasize at significantly higher rate, as compared to DC or RC melanomas.

By the analysis of the expression of several biomarkers, the molecular signature, and the biological behaviour *in vitro*, we have defined a specific bio-molecular profile for each RCM-melanoma subtype (Figure S6). The first step of melanoma progression is RGP, characterized by the proliferation of atypical melanocytes in the epidermis. This is followed by VGP, which consists of proliferating tumor cells in the dermis (Clark et al., 1969). In this context, Ki67-positive cells define tumor proliferation compartments in melanomas. Moreover, the correlation of Ki67 expression and MI is used as melanoma prognostic marker (Phyllis et al., 2006). The presence of proliferating cells in dermis and high MI in CT and DN suggests the more aggressiveness of this tumor compared to DC/RC subtypes. Additionally, the expression of a small fraction of Ki67 positive cells in the dermis in RC vs DC, suggests that RC is more advanced tumor than DC.

The expression of aggressiveness-biomarkers (MERTK, Nestin), as well as the high levels of *CXCL8* and *BIRC5* mRNA underlined the increase of aggressive features from DC to CT/DN melanomas, which was also confirmed by their proliferative capacity *in vitro*. Additionally, CT and DN were characterized by more elevated levels of ABCB5, in line with the chemo-resistance proprieties of these tumor types (Chartrain et al., 2012).

The progressive modulation of cancer-progression-associated genes, such as ECM-remodeling, angiogenesis and inflammation, from DC to CT melanoma strongly suggests the switch in term of aggressiveness between these tumor types. Consistently, SMAD and TGF-β-signaling, BMP-ligands, the modulation of specific adhesion-molecules and differentiation-associated genes strongly correlate with tumor aggressiveness and progression (Schlegel et al., 2013,

For Review Only

1
2
3
4
5
6
7
8
9
10
11
12
13
14
15
16
17
18
19
20
21
22
23
24
25
26
27
28
29
30
31
32
33
34
35
36
37
38
39
40
41
42
43
44
45
46
47
48
49
50
51
52
53
54
55
56
57
58
59
60

Caramel et al., 2013; Rusciano, 2000). Cancer-associated TF-gene expression involved in these pathways was significantly modulated between the different RCM-subtypes, indicating an increase of aggressiveness and invasive capacities between these tumor types. DC melanoma may represent a well-differentiated tumor with limited abilities of proliferation and invasion, as shown by the significantly low expression of tumor aggressiveness/invasiveness-associated genes. Conversely, since RC melanoma was characterized by both RGP and VGP, we speculate that it may present an intermediate degree of aggressiveness between the well-differentiated DC-type and the most invasive CT-DN melanomas. Giving these characteristics of RC, we speculate that the higher expression of HIF-1α in this melanoma-subtype could be necessary for the acquisition of the invasive proprieties and the need of new vascularization (Widmer et al., 2013). Moreover, the increased CD271 expression in RC could be instrumental in favoring its epidermis-to-dermis transition (Saltari et al., 2016).

TGF-β-superfamily signaling as well as the modulation of specific adhesion molecules and cytoskeletal regulation play an important role in promoting invasiveness *in vitro* (Schlegel et al., 2013, Caramel et al., 2013). We found a significant modulation of the genes associated to cytoskeletal regulation, cadherin and TGF-β signaling in RC vs DC melanomas, confirming the more aggressive behavior of RC vs DC subtype. Moreover, a substantial gene modulation related to integrin and cadherin signaling pathways and angiogenesis was observed in CT vs. RC melanomas. At the same time, a switch from E-cadherin to N-cadherin expression from DC to CT melanomas was detected.

Altogether, our results strongly suggest the existence of a close correlation between RCM-observed cell-morphology and tumor aggressiveness. Giving the slow-growing features of DC melanoma (Argenziano et al., 2010), it could represent the less aggressive type of melanoma. Conversely, a tumor that arises with a predominant RC population has a faster pattern of growth and a shorter time to invasion (Pellacani et al., 2014). Subsequently, melanoma cells may

For Review Only

1
2
3
4
5
6
7
8
9
10
11
12
13
14
15
16
17
18
19
20
21
22
23
24
25
26
27
28
29
30
31
32
33
34
35
36
37
38
39
40
41
42
43
44
45
46
47
48
49
50
51
52
53
54
55
56
57
58
59
60

undergo a de-differentiation step, creating less cohesive cells aggregated into the dermis, corresponding to CT melanoma (Longo et al., 2013), confirmed by the higher expression of stemness markers in this tumor-type vs. DC/RC melanomas.

The present study demonstrated that DN melanoma is a unique tumor subtype with peculiar features. Although CT melanomas may share some morphological characteristics, i.e., small cell dermal aggregates, called "cerebriform nests" (Pellacani et al, 2005), with DN-type, biomolecular markers are significantly different. In fact, DN melanomas showed Ki67-positive cells only in the dermis, without any epidermal change, and expressed highest levels of the MICs markers, indicating a more undifferentiated state. Moreover, DN were significant more invasive than CT *in vitro*, which was confirmed by the higher expression of α4/α7-integrin and N-cadherin, as compared to CT. Interestingly, DN cells were able to attach and growth only when seeded directly into the dermis in skin reconstructs. Accordingly, E-cadherin, an epithelial adhesion molecule (Van Roy et al., 2014), was scarcely detected in DN melanoma. The peculiar features of DN melanoma are coherent with the idea of the different origin of this tumor. It could probably originate directly from dermal stem cells without an epidermal-RGP (Zalaudek et al., 2008; Hoerter et al., 2012).

To summarize, we believe that there are at least two main melanoma subtypes: (i) the epidermal-origin type, which may arise as DC or RC type, with the potential to progress into the CT-type developing invasive clones morphologically similar to DN-type melanoma, but with different biomolecular profiles; and (ii) the dermal-origin type, characterized by DN morphology upon RCM and the most aggressive biomolecular profile, as expressed by higher level of MICs markers and higher expression of α4/α7-integrin and N-cadherin.

This work reports the most comprehensive study on the correlation between RCM-observed cell-morphology and bio-molecular behavior of melanoma, which accounts for diverse degree of tumor aggressiveness. Moreover, these data confirm that in vivo RCM can be a dependable

For Review Only

1 2 3 4 5 6 7 8 9 10 11 12 13 14 15 16 17 18 19 20 21 22 23 24 25 26 27 28 29 30 31 32 33 34 35 36 37 38 39 40 41 42 43 44 45 46 47 48 49 50 51 52 53 54 55 56 57 58 59 60

tool for detecting different types of melanoma and for screening purposes. The findings of the present study represent a first step to the creation of an integrated clinical/biomolecular model of melanoma classification for reaching a more accurate patient/tumor tailored therapeutic approach.

Materials and Methods

Melanoma lesions retrieval

Melanoma cases for retrospective study were retrieved from the database of the Department of Dermatology of the University of Modena and Reggio Emilia.

Melanoma biopsies were provided by the Dermatology Surgery of the Policlinic of Modena and Sassuolo Hospital. The use of melanoma biopsies was approved by the Ethical Committee of Area Vasta Emilia Nord (Prot. N. 475, Doc. 118/14 – 09/02/2016).

Inclusion criteria, immunohistochemistry, culture methods and *in vitro* assay were fully described in the supplementary materials.

NanoString and western blotting

Total-RNA was extracted from histological sections. NanoString and computational analysis was performed as described in supplementary materials. Total proteins were extracted from cryopreserved melanoma biopsies and Western blot was performed as indicated in supplementary materials.

Statistical analysis

Statistical analysis was performed using STATA® software 14 or GraphPad Prism 9 as indicated in supplementary materials. Data were considered significant with $p < 0.05$ (*), $p < 0.01$ (**) and $p < 0.001$ (***).

For Review Only

1
2
3
4
5
6
7
8
9
10
11
12
13
14
15
16
17
18
19
20
21
22
23
24
25
26
27
28
29
30
31
32
33
34
35
36
37
38
39
40
41
42
43
44
45
46
47
48
49
50
51
52
53
54
55
56
57
58
59
60

Data availability statement

Data supporting the findings of this study are available from the corresponding author upon reasonable request. Datasets related to this study can be found at [https://www.ncbi.nlm.nih.gov/geo/query/acc.cgi?acc=GSE174395] by using the following private token: qfohocyydbqvvst.

Conflict of interest

Authors declare no conflict of interest.

For Review Only

Founding

This work was supported by the AIRC grant IG 2015 (N. 16890).

Author contribution

A.M, F.F, C.P and G.P designed the study. M.Q., A.M. performed most of the experiments and data analysis. F.F, S.C. and G.P performed RCM analysis and enrolled patients. F.F., M.P., C.M. and A.M.C provide melanoma samples. L.F. performed immunohistochemical reaction. M.Q, A.M and C.V. performed immunohistochemical analyses. E.P. and M.Q. performed computational analysis. S.K. performed statistical analysis. M.Q., A.M. and C.P. wrote the manuscript. All authors contributed to drafting and revising the article to give final approval.

References

Argenziano G., Kittler H., Ferrara G., Rubegni P et al., Slow-growing melanoma: a dermoscopy follow-up study, Br J Dermatol., 161 (2010); pp. 267-73. doi: 10.1111/j.1365-2133.2009.09416.x.

Arrangoiz R., Dorantes J., Cordera F., Juarez M. M., Pequentin E. M. De Leon E. L. Melanoma Review: Epidemiology, Risck Factors, Diagnoses and Staging, Journal of Cancer Treatment and Research, 4 (2016); pp. 1-15. DOI: 10.11648/j.jctr.20160401.11

Beretti F., Bertoni L., Farnetani F., Pellegrini C., Gorelli G., Cesinaro A.M., et al., Melanoma types by in vivo reflectance confocal microscopy correlated with protein and molecular genetic alterations: A pilot study, EXP Dermatol., 28 (2019); pp. 254-260. DOI: 10.1111/exd.13877.

Boiko A. D., O. V. Razorenova, M. Van De Rijn et al., Human melanoma-initiating cells express neural crest nerve growth factor receptor CD271, Nature, 466 (2010); pp. 133–137, 2010. DOI: 10.1038/nature09161

Bosserhoff A. K. , Ellmann L., Quast A. S., et al., Loss of T-cadherin (CDH-13) regulates AKT signaling and desensitizes cells to apoptosis in melanoma, 53 (2013); pp. 635-47. DOI: 10.1002/mc.22018

Broekaert S.M.C., Roy R., Okamoto I., et al., Genetic and morphologic features for melanoma classification., Pigment Cell Melanoma Res., 23 (2010); pp. 763-770. DOI: 10.1111/j.1755-148X.2010.00778.x

Caramel J, Papadogeorgakis E, Hill L, Browne GJ et al., A switch in the expression of embryonic EMT-inducers drives the development of malignant melanoma *Cancer Cell*, 14 (2013); pp. 466-80. DOI: 10.1016/j.ccr.2013.08.018.

Chartrain M, Riond J, Stennevin A, Vandenberghe I, Gomes B, Lamant L, et al., Melanoma chemotherapy leads to the selection of ABCB5-expressing cells., PLoS One, 7 (2012). DOI: 10.1371/journal.pone.0036762

Clark W H, From L, Bernardino E A. The histogenesis and biologic behavior of primary human malignant melanoma of the skin. Cancer Res, 29 (1969); pp. 705-27.

For Review Only

1
2
3
4
5
6
7
8
9
10
11
12
13
14
15
16
17
18
19
20
21
22
23
24
25
26
27
28
29
30
31
32
33
34
35
36
37
38
39
40
41
42
43
44
45
46
47
48
49
50
51
52
53
54
55
56
57
58
59
60

Eskens FA, Dumez H, Hoekstra R, et l., Phase I and pharmacokinetic study of continuous twice weekly intravenous administration of Cilengitide (EMD 121974), a novel inhibitor of the integrins alphavbeta3 and alphavbeta5 in patients with advanced solid tumours., Eur J Cancer., 39 (2003); pp. 917-26. DOI: 10.1016/s0959-8049(03)00057-

Fink C. and Haenssle., Non –invasive tools for the diagnosis of cutaneous melanoma., Skin Reasearch and Technology, 3 (2016); pp. 261.271. DOI: 10.1111/srt.12350

Gajos-Michniewicz A. and Malgorzata C., WNT signaling in melanoma., Int. J. Mol. Sci., 9 (2020); pp. 4852. DOI: 10.3390/ijms21144852.

Graf S. A., Busch C., Bosserhoff A.K., et al., SOX10 Promotes Melanoma Cell Invasion by Regulating Melanoma Inhibitory Activity, J. Invest. Dermatology., 134 (2014), pp. 2212-2220. DOI: 10.1038/jid.2014.128.

Grazziotin TC., Alarcon I., Bonamigo RR., Carrera C., Potrony M., Auguilera P., Puig-Butillé J-A., Brito J., Badenas C., Alòs L., Malvehy J., Puig S., Association between confocal morphologic classification and clinical phenotypes of multiple primary and familial melanomas, JAMA Dermatology, 152 (2016); pp. 1099-1105. DOI: 10.1001/jamadermatol.2016.1189

Haass NK, Smalley KS, Li L, Herlyn M., Adhesion, migration and communication in melanocytes and melanoma., Pigment Cell Res., 18 (2005); pp. 150–159. DOI: 10.1111/j.1600-0749.2005.00235.x.

Hoerter J., Bradley P., Casillas A., et al., Extrafollicular dermal melanocyte stem cells and melanoma., Stem Cells Int (2012). DOI: 10.1155/2012/407079.

Javelaud D, Alexaki VI, Mauviel A., Transforming growth factor-beta in cutaneous melanoma., Pigment Cell Melanoma Res., 21 (2008); pp. 123–132.

Klein WM, Wu BP, Zhao S, et al., Increased expression of stem cell markers in malignant melanoma., Mod Pathol, 20 (2007); pp. 102–107. DOI: 10.1038/modpathol.3800720.

For Review Only

1
2
3
4
5
6
7
8
9
10
11
12
13
14
15
16
17
18
19
20
21
22
23
24
25
26
27
28
29
30
31
32
33
34
35
36
37
38
39
40
41
42
43
44
45
46
47
48
49
50
51
52
53
54
55
56
57
58
59
60

Longo C, Farnetani F, Ciardo S et al. Is confocal microscopy a valuable tool in diagnosing nodular lesions? A study of 140 cases., Br J Dermatol., 169 (2013); pp. 58-67. DOI: 10.1111/bjd.12259

Monzani E., F. Facchetti, E. Galmozzi et al., “Melanoma contains CD133 and ABCG2 positive cells with enhanced tumourigenic potential, European Journal of Cancer, 43 (2007); pp. 935–946. DOI: 10.1016/j.ejca.2007.01.017

Pellacani G., De Pace B., Reggiani C., Cesinaro AM., Argenziano G., Zalaudek I., Soyer H.P., Longo C. Distinct melanoma types based on reflectance confocal microscopy. Experimental Dermatology, 2014. DOI: 10.1111/exd.12417.

Pellacani G, Guitera P, Longo C, et al. The impact of in vivo reflectance confocal microscopy for the diagnostic accuracy of melanoma and equivocal melanocytic lesions., J Invest Dermatol. 127 (2007); pp. 2759-2765. DOI: 10.1038/sj.jid.5700993

Pellacani G, Cesinaro AM, Seidenari S. In vivo assessment of melanocytic nests in nevi and melanomas by reflectance confocal microscopy., Mod Pathol., 18 (2005); pp. 469-74 DOI: 10.1038/modpathol.3800330

Phyllis A. Gimotty, Patricia Van Belle, David E. Elder, et al., Biologic and Prognostic Significance of Dermal Ki67 Expression, Mitoses, and Tumorigenicity in Thin Invasive Cutaneous Melanoma., Journal of Clinical Oncology, 13 (2006); pp.8048-8056. DOI: 10.1200/JCO.2005.02.0735

Rajadhyaksha M, Grossman M, Esterowitz D, et al. In vivo confocal scanning laser microscopy of human skin: melanin provides strong contrast., J Invest Dermatol., 104 (1995); pp. 946-952. DOI: 10.1111/1523-1747.ep12606215

Ramakrishnan V., Bhaskar V., Law D. A., et al., Preclinical evaluation of an anti-alpha5beta1 integrin antibody as a novel anti-angiogenic agent., J Exp Ther Oncol., 5 (2006); pp. 273-86.

For Review Only

1
2
3
4
5
6
7
8
9
10
11
12
13
14
15
16
17
18
19
20
21
22
23
24
25
26
27
28
29
30
31
32
33
34
35
36
37
38
39
40
41
42
43
44
45
46
47
48
49
50
51
52
53
54
55
56
57
58
59
60

Richmond A., Yang J., and Su Y., The good and the bad of chemokines/chemokine receptors in Melanoma., *Pigment Cell Melanoma Res*., 22 (2009); pp. 175–186. DOI:10.1111/j.1755-148X.2009.00554.x.

Rodriguez-Cerdeira C., Gregorio M. C., Lopez-Barcenas A. et al., Advances in Immunotherapy for Melanoma: A Comprehensive Review, Mediat Inflamm., 207 (2017); pp.1-14. DOI: 10.1155/2017/3264217

Rusciano, D. Differentiation and metastasis in melanoma. Crit. Rev. Oncog., 11 (2000); pp. 147–163.

Saltari A., Truzzi F., Quadri M., Lotti R., Palazzo E. et al., CD271 Down-Regulation Promotes Melanoma Progression and Invasion in Three-Dimensional Models and in Zebrafish, J. Invest. Dermatol., 136 (2016); pp.2049-2058. DOI: 10.1016/j.jid.2016.05.116.

Santini R, Pietrobono S, Pandolfi S, Montagnani V, D'Amico M, Penachioni JY et al., SOX2 regulates self-renewal and tumorigenicity of human melanoma-initiating cells., Oncogene, 33 (2014); pp. 4697–4708. DOI: 10.1038/onc.2014.71.

Schlegel J., Sambada M.J, Sather S. eta al., MERTK receptor tyrosine kinase is a therapeutic target in melanoma., J Clin Investigation, 123 (2013): pp. 2257-2267. DOI: 10.1172/JCI67816.

Schlegel NC, von Planta A, Widmer DS, Dummer R, Christofori G. PI3K signalling is required for a TGFβ-induced epithelial-mesenchymal-like transition (EMT-like) in human melanoma cells., Exp Dermatol., 24 (2015); pp.22–28. DOI: 10.1111/exd.12580

Scolyer R.A., Long G. V., Thompson J.F.; Evolving concepts in melanoma classification and their relevance to multidisciplinary melanoma patient care., Molecular Oncology (2011); pp. 124-136. DOI: 10.1016/j.molonc.2011.03.002.

1 2 3 4 5 6 7 8 9 10 11 12 13 14 15 16 17 18 19 20 21 22 23 24 25 26 27 28 29 30 31 32 33 34 35 36 37 38 39 40 41 42 43 44 45 46 47 48 49 50 51 52 53 54 55 56 57 58 59 60

Takeuchi H., Morton D. L., Elashoff D., Hoon D. S. B., Survivin expression by metastatic melanoma predicts poor disease outcome in patients receiving adjuvant polyvalent vaccine. Int. J. Cancer, 117 (2005), pp.1032–1038. DOI: 10.1002/ijc.21267

Thompson J.F., Scolyer R.A., and Kefford R.F. Cutaneous melanoma., Lancet, 365 (2005); pp. 687-701. DOI: 10.1016/S0140-6736(05)17951-3

Ugurel S, Rappl G, Tilgen W, Reinhold U., Increased serum concentration of angiogenic factors in malignant melanoma patients correlates with tumor progression and survival., J. Clin. Oncol., 19 (2001); pp. 577–583. DOI: 10.1200/JCO.2001.19.2.577

Van Roy F., Beyond E-cadherin: roles of other cadherin superfamily members in cancer., Nat Rev Cancer, 14 (2014); pp. 121–34. DOI: 10.1038/nrc3647.

Whiteman D.C., Pavan W.J., Boris C. and Bastian C., The melanomas: a synthesis of epidemiological, clinical, histopathological, genetic, and biological aspects, supporting distinct subtypes, casual pathways, and cells of origin, Pigment Cell Melanoma Res. 24 (2011); pp. 879-897. DOI: 10.1111/j.1755-148X.2011.00880.x.

Widmer D.S., Hoek K., Cheng D.S., Eichhoff O. M., Biedermann T., et al., Hypoxia contributes to melanoma heterogeneity by triggering HIF1α-dependent phenotype switching., J. Invest Dermatol., 133 (2013); pp. 2436-2443 DOI: 10.1038/jid.2013.115

Zalaudek I., Marghoob A. A., Scope A., et al., Three roots of melanoma., Arch Dermatol., 144 (2008); pp. 1375-9. DOI: 10.1001/archderm.144.10.1375.

Table

Table 1. Association between RCM melanoma subtypes and clinical characteristics.

		DC (n=25)		RC (n=25)		DN (n=15)		CT (n=25)		Total		p-value
Age, mean ±SD (Range)		69.2 ±12.2 (47-88)		52.6 ±15.9 (30-89)		55.6 ±15.3 (31-78)		64 ±18.2 (24-90)		60.9 ±16.8 (24-90)		0.001
		N	%	N	%	N	%	N	%	N	%	p-value
Sex												
	Female	8	32.0	12	48.0	7	46.7	8	32.0	35	38.9	0.521
	Male	17	68.0	13	52.0	8	53.3	17	68.0	55	61.1	
Tumor type												
	RGP	23	92.0	14	56.0	1	6.7	1	4.0	39	43.3	<0.001
	VGP	2	8.0	11	44.0	14	93.3	24	96.0	51	56.7	
Tumor site												
	Arts	4	16.0	10	40.0	8	53.3	10	40.0	32	35.6	0.022
	Face	7	28.0	0	0.0	1	6.7	2	8.0	10	11.1	
	Trunk	14	56.0	15	60.0	6	40.0	13	52.0	48	53.3	
BRAF ^{V600E}		6	24.0	18	72.0	7	46.6	14	56.0	45	51.1	0.007
BRESLOW,n, mean ±SD(Range)		25, 0.2 ±0.3 (0-1.04)		25, 0.6 ±0.4 (0-2)		15, 5.8 ±7.1 (0.65-24)		25, 2.6 ±2.0 (0.5-8)		88, 2.0 ±3.6 (0-24)		<0.001
Breslow Index		N	%	N	%	N	%	N	%	N	%	
	mm≤1	24	96.0	22	88.0	1	6.7	5	20.0	50	55.6	<0.001
	1<mm≤2	1	4.0	3	12.0	3	20.0	8	32.0	15	16.7	
	2<mm≤4	0	0.0	0	0.0	6	40.0	7	28.0	13	14.4	
	5<mm≤10	0	0.0	0	0.0	2	13.3	0	0.0	2	2.2	
	mm>10	0	0.0	0	0.0	3	20.0	5	20.0	8	8.9	
Clark Level												
	I	11	44.0	1	4.0	0	0.0	0	0.0	12	13.3	<0.001
	II	11	44.0	12	48.0	1	6.7	1	4.0	25	27.8	
	III	3	12.0	10	40.0	5	33.3	8	32.0	26	28.9	
	IV	0	0.0	2	8.0	7	46.7	13	52.0	22	24.4	
	V	0	0.0	0	0.0	2	13.3	3	12.0	5	5.6	
Mitotic Index												
	0-1	24	96.0	24	96.0	5	33.3	9	36.0	60	66.7	<0.001
	2-5	1	4.0	1	4.0	7	46.7	10	40.0	19	21.1	
	>5	0	0.0	0	0.0	3	20.0	6	24.0	9	10.0	
Previous history of M		9	36.0	2	8.0	1	6.7	0	0.0	12	13.3	0.001
Posive sentinel lymph node		0	0.0	2	8.0	4	26.7	8	32.0	14	15.6	0.013
Follow up												
Relaps or new M		10	40.0	2	8.0	4	26.7	3	12.0	17	18.9	0.118
Metastasis 0-5 years		0	0.0	1	4.0	5	33.3	5	20.0	11	12.2	0.005

For Review Only

1
2
3 Abbreviation: DC, Dendritic cell melanoma; RC, Round cell melanoma; CT, Combined type
4
5 melanoma; DN, Dermal Nest Melanoma; M, Melanoma; SD, Standard Deviation; N, Number;
6
7
8 RGP, Radial Growth Phase; VGP, Vertical Growth Phase.
9
10
11
12
13
Figure Legends

14
15 **Figure 1. Representative clinical, histopathological and RCM images of melanoma**
16
17 **subtype**. DC: **a, b**) Clinical and Dermoscopic image of Lentigo Maligna (LM). **c**) RCM
18
19
20 image of melanoma in the transition from epidermis to DEJ shows numerous lines
21
22 corresponding to dendritic cells (red rectangle and red arrows), coming out of the hair
23
24 follicles (asterisk). (**d-f**) Hematoxylin and eosin (H&E), HMB45 and Melan-A staining.
25
26
27 Scale bar 50µm. RC: **a-b**) Clinical and Dermoscopic image of Melanoma. **c**) RCM shows
28
29 the presence of several roundish large melanocytes (red rectangle and red arrows) with
30
31 bright cytoplasm and hypo-reflective nucleus. **d-f**) H&E and HMB45, Melan-A staining.
32
33
34 Scale bar 50µm. CT: **a-b**) Clinical and Dermoscopic image of Melanoma. **c**) RCM shows
35
36 the presence of dendritic cells, roundish cells (red rectangle and red arrows) and
37
38 polymorphic cells (green arrow) within the dermal papilla. **d-f**) H&E and HMB45,
39
40
41 Melan-A staining. Scale bar 50µm. DN: **a-b**) Clinical and Dermoscopic image of
42
43 Melanoma. **c**) RCM shows the presence of a cerebriform nesting (red rectangle and red
44
45 arrows) located at the dermal level. **d-f**) H&E, HMB45 and Melan-A staining. Scale bar
46
47
48 500µm.
49
50
51
52
53 **Figure 2. Correlation between RCM melanoma subtypes to markers expression and**
54
55 **biological behaviour in vitro**. (**a**) The expression of Ki67, MERTK, Nestin, Hif-1α, ABCB5
56
57 and (**b**) SOX-10, SOX-2, CD133 and CD271 were evaluated by IHC. Protein expression was
58
59 scored 0 to 4 and the average positive cells was calculated for each individual melanoma as
60

For Review Only

1
2
3
4
5
6
7
8
9
10
11
12
13
14
15
16
17
18
19
20
21
22
23
24
25
26
27
28
29
30
31
32
33
34
35
36
37
38
39
40
41
42
43
44
45
46
47
48
49
50
51
52
53
54
55
56
57
58
59
60

follow: 0 score, 0% staining melanoma cells; 1=1%-25% staining positive melanoma cells; 2=26%-50% staining positive melanoma cells; 3=51-75% staining-positive melanoma cells and 4=76%-100% staining positive melanoma cells. Scale bar 50µm. (**c**) Melanoma biopsies were digested and approximately 10^4 cells were seeded for spheroid formation. (**d**) Total spheroids area was measured by ImageJ software and (**e**) MTT assay was performed at different time points.

Figure 3. Gene expression profile of RCM melanoma subtypes. (a) Heatmaps representing **t**he main GO BP terms identified by DAVID Functional Association Tool. Gene expression values for each heatmap were ranked according to their z-score after normalization. The gene expression was showed as raw value of normalized intensity. (**b**) Differently expressed genes were uploaded onto Venny 2.1 tool. RC, CT and DN melanomas were compared to DC melanoma (Venny diagram on the left). The gene list resulting modulated in each group obtained from Venny were uploaded on PANTHER Classification System. The five more significant modulated pathways were reported in (**b**) upregulated and (**c)** downregulated pathways: 1) RC vs DC, 2) CT vs DC, 3) DN vs DC and 4) common up or down regulated pathways. (**d**) The expression levels of *BIRC5* (Survivin), CXCL8 and *NGFR* (CD271) mRNA were evaluated by Real-Time PCR in each RCM-melanoma subtype.

For Review Only

Figure 4. Correlation between RCM-observed morphology and tumor aggressiveness. (a) Up and down regulated genes in RC vs DC comparison were uploaded on PANTHER Classification System. The five more significant modulated pathways were reported in: 1) upregulated and 2) downregulated pathways. Graphs on the right represent the fold change of each gene clustered on the base of the pathway involved. (**b**) CT vs RC differently expressed genes were uploaded on PANTHER Classification System. Genes were clustered based on the

main significative pathway involved: 1) upregulated and 2) downregulated pathways. Graphs on the right represent the fold change of each gene clustered on the base of the pathway involved. (**c**) DC, RC, and CT melanoma samples were retrieved. HMB45 and CD271 expression were evaluated by IHC. Scale bar 50μm. (**d**) Correlation between Breslow index and CD271 expression level. (**e**) Proteins were extracted from DC, RC, and CT melanoma biopsies and immunoblotting for E and N-cadherin was performed, using β-actin as normalizing protein.

Figure 5. Differences between the most aggressive RCM-melanoma subtypes. (**a**) Up and downregulated genes in CT vs DN comparison was uploaded on PANTHER Classification System. Genes were clustered based on the main significative pathway involved: 1) upregulated and 2) downregulated pathways. Graphs on the right represent the fold change of each gene clustered on the base of the pathway involved. (**b**) CT and DN spheroids were transferred in a type I collagen matrix and pictures were taken at different time. (**c**) Total spheroids area (**d**) the percentage of fragmentation and (**e**) cells invading area were evaluated by ImageJ softwar. (**f**) the invasion distance reached by cells from spheroids were measured by GIMP software. (**g**) CT and DN cells were employed to reconstruct melanoma skin equivalent. After 14 days of emersion conditions, melanoma skin equivalents were paraffin embedded and sections were stained with H&E, Melan-A and HMB45 by IHC. Scale Bar 50 □m. (**h**) The expression of MIB/Ki67, E and N-cadherin, α_7-integrin, α_4-integrin, and SOX-2 were revealed by IF and measured by ImageJ software. (**i**) DN spheroids were transferred in a type I collagen matrix and, after 336h, fixed with PFA 4%. The expression of α_4-integrin (red) and CD271 (green) were revealed by IF. Scale Bar 100 □m.

For Review Only

1
2
3
4
5
6
7
8
9
10
11
12
13
14
15
16
17
18
19
20
21
22
23
24
25
26
27
28
29
30
31
32
33
34
35
36
37
38
39
40
41
42
43
44
45
46
47
48
49
50
51
52
53
54
55
56
57
58
59
60

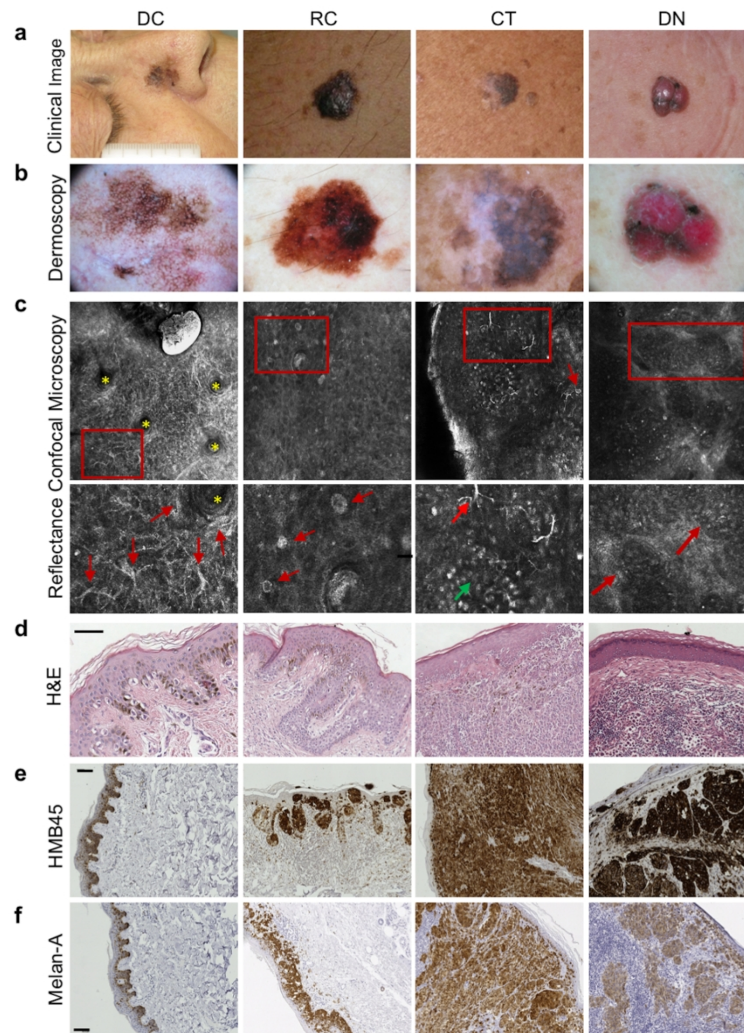

Figure 1. Representative clinical, histopathological and RCM images of melanoma subtype. DC: a, b) Clinical and Dermoscopic image of Lentigo Maligna (LM). c) RCM image of melanoma in the transition from epidermis to DEJ shows numerous lines corresponding to dendritic cells (red rectangle and red arrows), coming out of the hair follicles (asterisk). (d-f) Hematoxylin and eosin (H&E), HMB45 and Melan-A staining. Scale bar 50um. RC: a-b) Clinical and Dermoscopic image of Melanoma. c) RCM shows the presence of several roundish large melanocytes (red rectangle and red arrows) with bright cytoplasm and hypo-reflective nucleus. d-f) H&E and HMB45, Melan-A staining. Scale bar 50um. CT: a-b) Clinical and Dermoscopic image of Melanoma. c) RCM shows the presence of dendritic cells, roundish cells (red rectangle and red arrows) and polymorphic cells (green arrow) within the dermal papilla. d-f) H&E and HMB45, Melan-A staining. Scale bar 50um. DN: a-b) Clinical and Dermoscopic image of Melanoma. c) RCM shows the presence of a cerebriform nesting (red rectangle and red arrows) located at the dermal level. d-f) H&E, HMB45 and Melan-A staining. Scale bar 50um.

180x220mm (300 x 300 DPI)

1
2
3
4
5
6
7
8
9
10
11
12
13
14
15
16
17
18
19
20
21
22
23
24
25
26
27
28
29
30
31
32
33
34
35
36
37
38
39
40
41
42
43
44
45
46
47
48
49
50
51
52
53
54
55
56
57
58
59
60

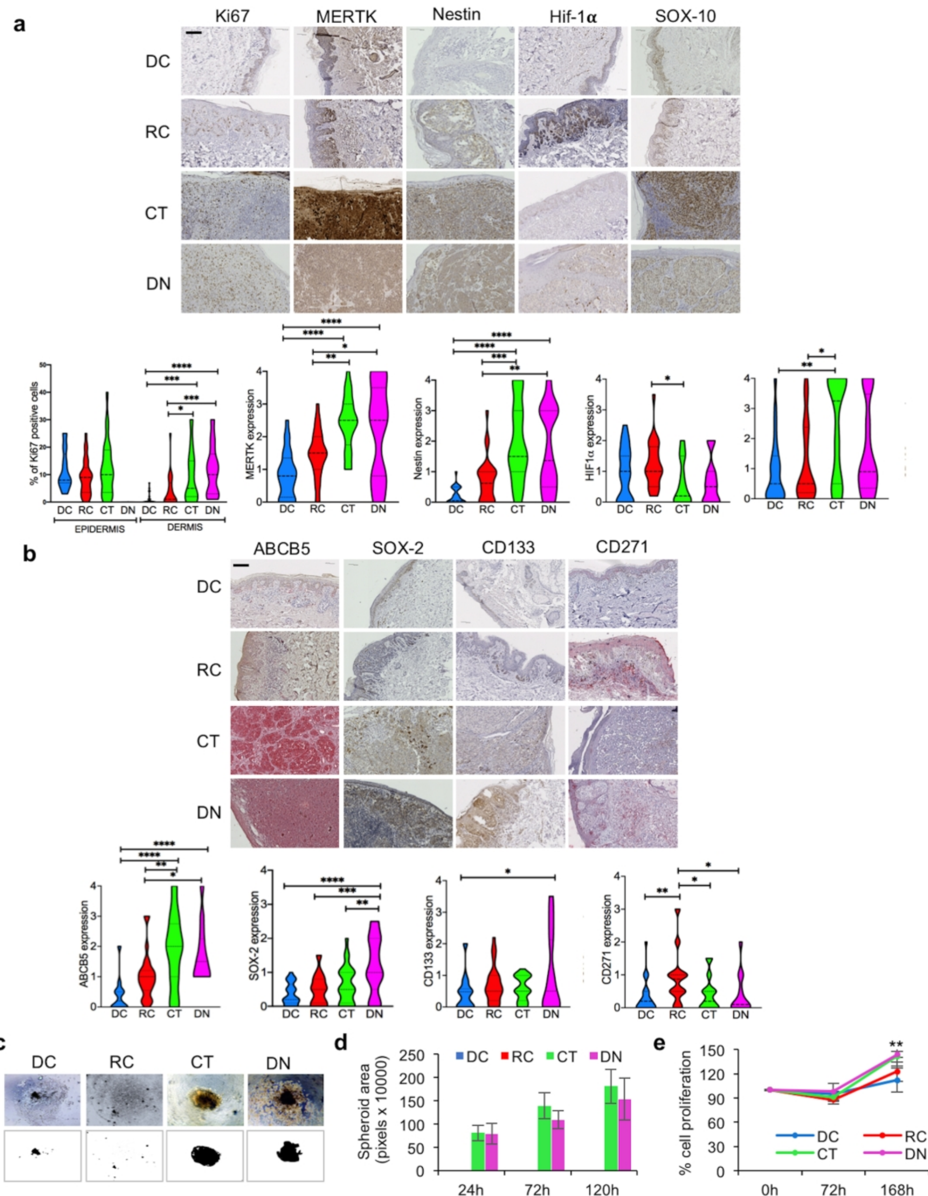

Figure 2. Correlation between RCM melanoma subtypes to markers expression and biological behaviour in vitro. (a) The expression of Ki67, MERTK, Nestin, Hif-1α, ABCB5 and (b) SOX-10, SOX-2, CD133 and CD271 were evaluated by IHC. Protein expression was scored 0 to 4 and the average positive cells was calculated for each individual melanoma as follow: 0 score, 0% staining melanoma cells; 1=1%-25% staining positive melanoma cells; 2=26%-50% staining positive melanoma cells; 3=51-75% staining-positive melanoma cells and 4=76%-100% staining positive melanoma cells. Scale bar 50um. (c) Melanoma biopsies were digested and approximately 104 cells were seeded for spheroid formation. (d) Total spheroids area was measured by ImageJ software and (e) MTT assay was performed at different time points.

180x220mm (300 x 300 DPI)

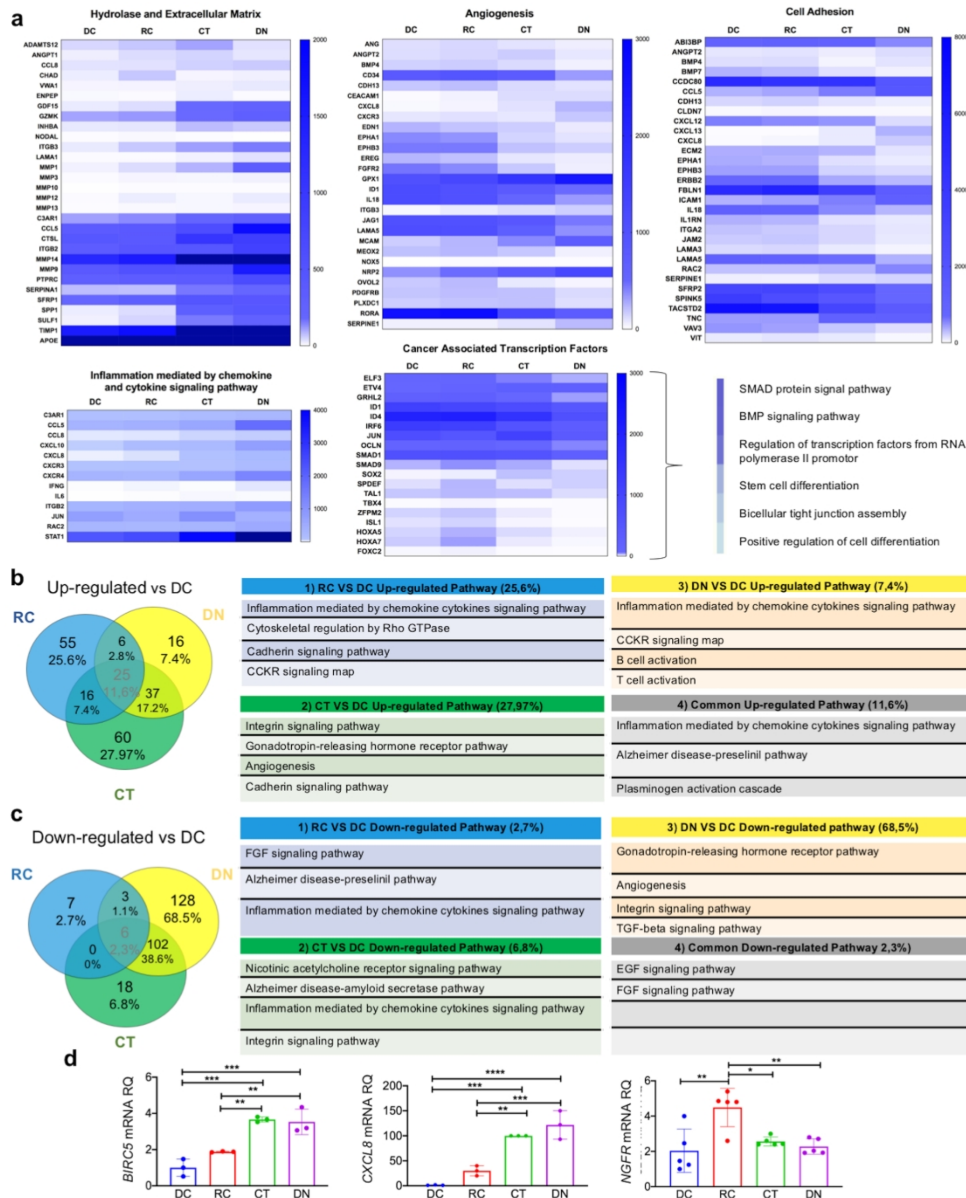

Figure 3. Gene expression profile of RCM melanoma subtypes. (a) Heatmaps representing the main GO BP terms identified by DAVID Functional Association Tool. Gene expression values for each heatmap were ranked according to their z-score after normalization. The gene expression was showed as raw value of normalized intensity. (b) Differently expressed genes were uploaded onto Venny 2.1 tool. RC, CT and DN melanomas were compared to DC melanoma (Venny diagram on the left). The gene list resulting modulated in each group obtained from Venny were uploaded on PANTHER Classification System. The five more significant modulated pathways were reported in (b) upregulated and (c) downregulated pathways: 1) RC vs DC, 2) CT vs DC, 3) DN vs DC and 4) common up or down regulated pathways. (d) The expression levels of BIRC5 (Survivin), CXCL8 and NGFR (CD271) mRNA were evaluated by Real-Time PCR in each RCM-melanoma subtype.

179x220mm (300 x 300 DPI)

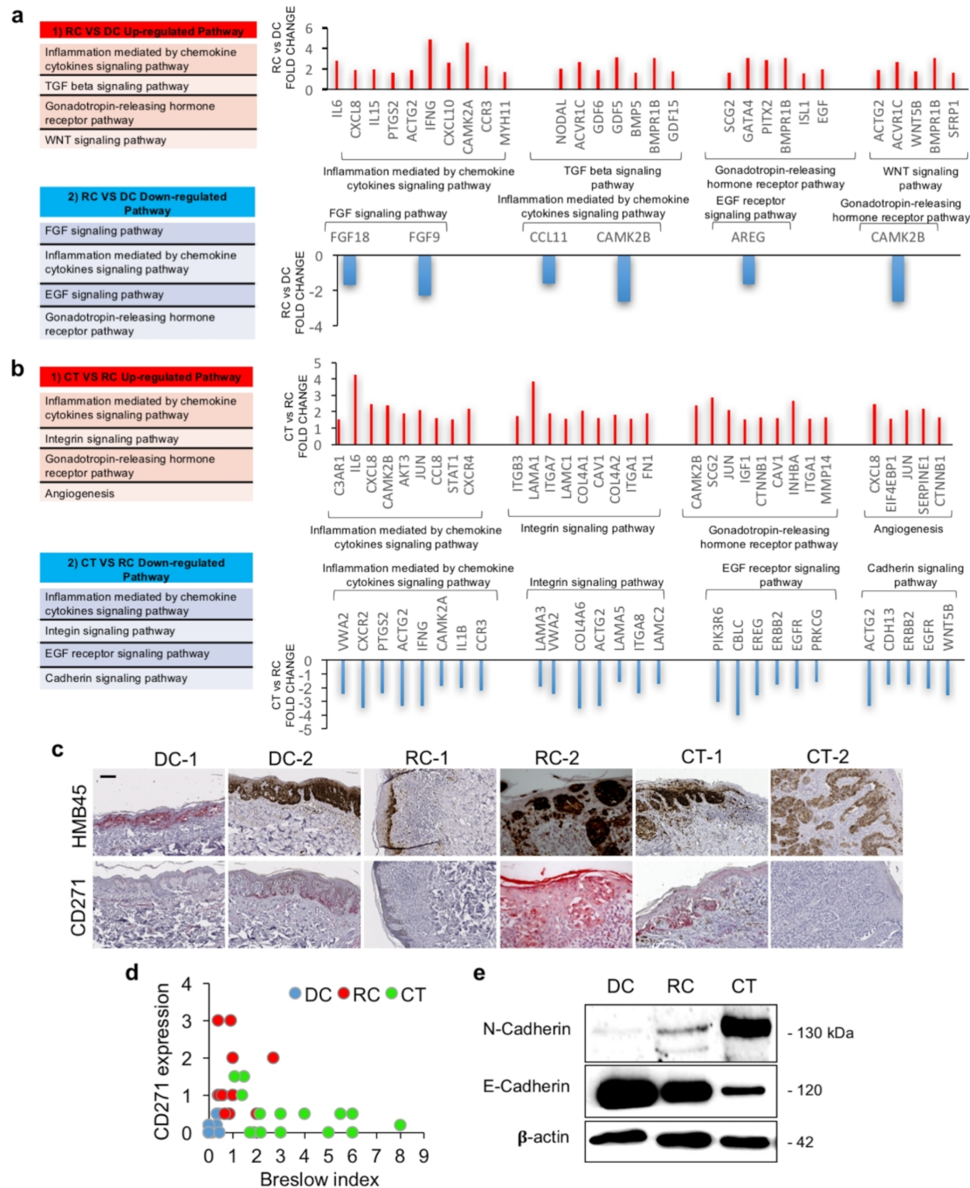

Figure 4. Correlation between RCM-observed morphology and tumor aggressiveness. (a) Up and down regulated genes in RC vs DC comparison were uploaded on PANTHER Classification System. The five more significant modulated pathways were reported in: 1) upregulated and 2) downregulated pathways. Graphs on the right represent the fold change of each gene clustered on the base of the pathway involved. (b) CT vs RC differently expressed genes were uploaded on PANTHER Classification System. Genes were clustered based on the main significative pathway involved: 1) upregulated and 2) downregulated pathways. Graphs on the right represent the fold change of each gene clustered on the base of the pathway involved. (c) DC, RC, and CT melanoma samples were retrieved. HMB45 and CD271 expression were evaluated by IHC. Scale bar 50um. (d) Correlation between Breslow index and CD271 expression level. (e) Proteins were extracted from DC, RC, and CT melanoma biopsies and immunoblotting for E and N-cadherin was performed, using β-actin as normalizing protein.

180x220mm (300 x 300 DPI)

1
2
3
4
5
6
7
8
9
10
11
12
13
14
15
16
17
18
19
20
21
22
23
24
25
26
27
28
29
30
31
32
33
34
35
36
37
38
39
40
41
42
43
44
45
46
47
48
49
50
51
52
53
54
55
56
57
58
59
60

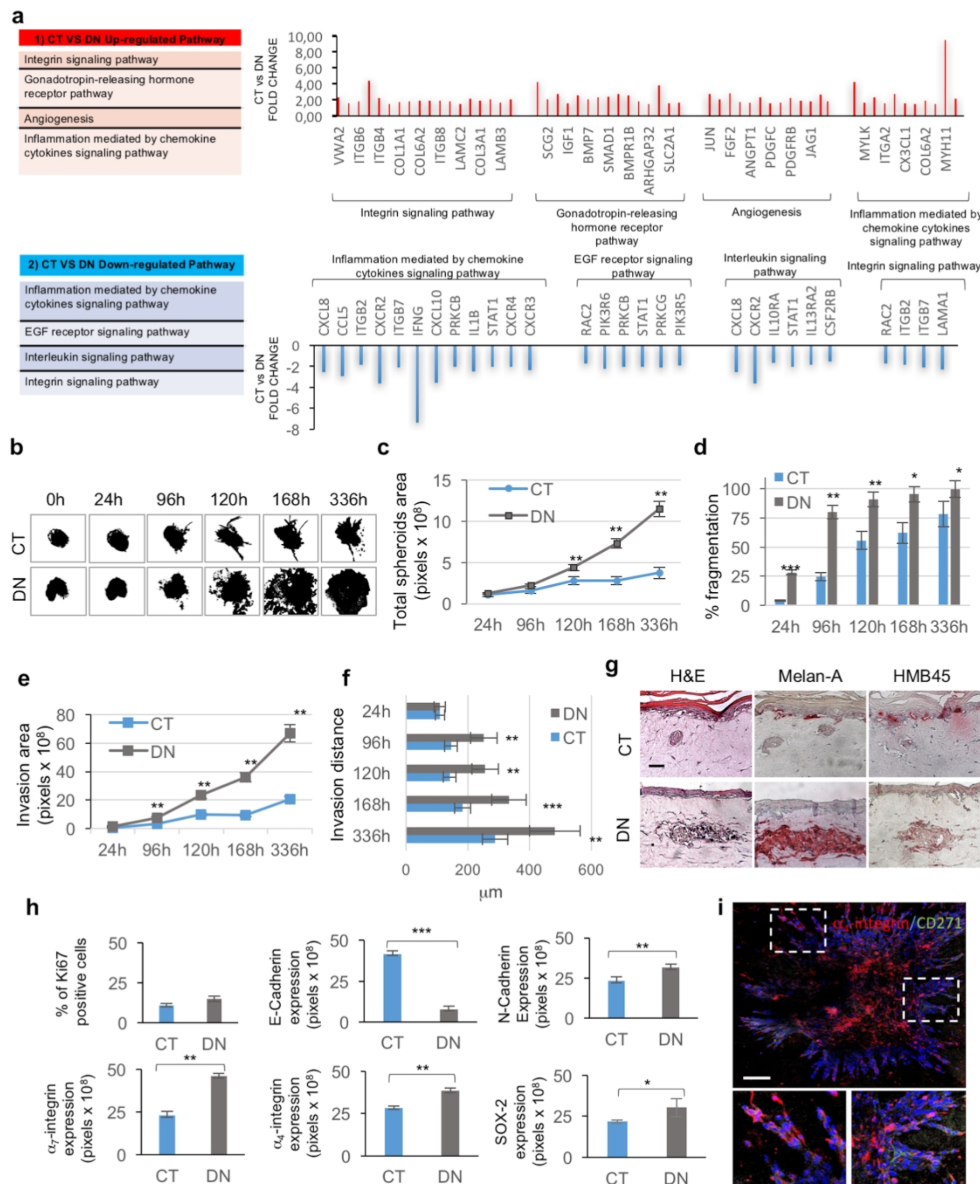

Figure 5. Differences between the most aggressive RCM-melanoma subtypes. (a) Up and downregulated genes in CT vs DN comparison was uploaded on PANTHER Classification System. Genes were clustered based on the main significative pathway involved: 1) upregulated and 2) downregulated pathways. Graphs on the right represent the fold change of each gene clustered on the base of the pathway involved. (b) CT and DN spheroids were transferred in a type I collagen matrix and pictures were taken at different time. (c) Total spheroids area (d) the percentage of fragmentation and (e) cells invading area were evaluated by ImageJ softwar. (f) the invasion distance reached by cells from spheroids were measured by GIMP software. (g) CT and DN cells were employed to reconstruct melanoma skin equivalent. After 14 days of emersion conditions, melanoma skin equivalents were paraffin embedded and sections were stained with H&E, Melan-A and HMB45 by IHC. Scale Bar 50 um. (h) The expression of MIB/Ki67, E and N-cadherin, α7-integrin, α4-integrin, and SOX-2 were revealed by IF and measured by ImageJ software. (i) DN spheroids were transferred in a type I collagen matrix and, after 336h, fixed with PFA 4%. The expression of α4-integrin (red) and CD271 (green) were revealed by IF. Scale Bar 100 um.

1
2
3
4
5
6
7
8
9
10
11
12
13
14
15
16
17
18
19
20
21
22
23
24
25
26
27
28
29
30
31
32
33
34
35
36
37
38
39
40
41
42
43
44
45
46
47
48
49
50
51
52
53
54
55
56
57
58
59
60

180x220mm (300 x 300 DPI)

1
2
3
4
5
6
7
8
9
10
11
12
13
14
15
16
17
18
19
20
21
22
23
24
25
26
27
28
29
30
31
32
33
34
35
36
37
38
39
40
41
42
43
44
45
46
47
48
49
50
51
52
53
54
55
56
57
58
59
60

SUPPLEMETARY MATERIALS

Materials and Methods

Melanoma lesion retrieval

Melanoma cases were retrieved from the database of the Department of Dermatology of the University of Modena and Reggio Emilia. Inclusion criteria were: 1) confirmed diagnoses of melanoma, 2) availability of relevant clinical data in patient records and 3) histological, dermoscopic and confocal images.

Clinical, dermoscopic and RCM images were acquired through a Canfield Nikon D90 Digital SLR®, a Canfield Close-up Scale® (Canfield Imaging Systems, Fairfield, NJ, USA) and an RCM laser scanning microscope (Vivascope 1500®; MAVIG GmbH, Munich, Germany), respectively, and were stored in a dedicated database. RCM employs an 830nm laser beam with a maximum power of 20mW. Instrument and acquisition procedures were previously described (Rajadhyaksha et al., 1999; Pellacani et al., 2007). A minimum of 3 mosaics were obtained per lesion at 3 different depths, corresponding to the superficial epidermal layer (the stratum granulosum/spinosum), dermal-epidermal junction (DEJ), and papillary dermis. Each image was blindly evaluated by expert dermatologist for epidermal, DEJ and upper dermis architecture and classified into four melanoma subtypes, as previously reported (Pellacani et al., 2014).

For Review Only

Immunohistochemistry (IHC)

Melanoma markers were detected using UltraView Universal DAB and RED detection Kit (Ventana Medical Systems, Roche diagnostics International AG, Rotkreuz, Switzerland); except for BRAF mutation and CD271. The Opti-View DAB IHC detection kit were used to detect BRAF mutation (Ventana Medical Systems), while Fast Red kit UltraVision LP Detection System AP Polymer & Fast Red Chromogen (Thermo Fisher Scientific, Waltham, MA, USA) was used to detect CD271,

according to the manufacturer's protocol. Primary antibodies were listed in Supplementary Table S1. Images of the H&E and IHC-staining were obtained by a D-Sight slide scanner (Menarini Diagnostics, Firenze, Italy).

Melanoma biopsies digestion and culture methods

Melanoma biopsies were provided by the Dermatology Surgery of the Policlinic of Modena and Sassuolo Hospital. The use of melanoma biopsies was approved by the Ethical Committee of Area Vasta Emilia Nord (Prot. N. 475, Doc. 118/2014 – 09/02/2016). Biopsies was digested in a mix of collagenase I and IV (1:2000 and 1:500, respectively) (Gibco, Thermo Fisher Scientific) and cells were seeded and cultured using hanging drop or liquid overlay methods in RMPI medium supplemented with 10% of heat-inactivated serum, 2% of L-Glutamine and 1% of Penicillin/Streptomycin (Lonza, Basel, Switzerland).

MTT assay was performed to evaluate RCM-melanoma spheroids from 24 hours to 168 hours. Collagen invasion assay was used to assess the invasion ability of melanoma cells within a collagen I matrix. The area occupied by melanoma spheroids and the invasive capacity of cells were evaluated by ImageJ program (NIH), as previously indicated (Saltari et al., 2016).

NanoString and computational analyses

Total RNA was extracted from Formalin-Fixed Paraffin-Embedded samples by using RNeasy FFPE kit (Quiagen, Hilden, Germany), following the manufacturer's instruction. 32 samples were employed (9 for DC, 6 for RC, 7 for DN and 10 for CT). 10 slices of 10uM per patients were employed and only tumoral area was collected. cDNA was prepared using the High-Capacity cDNA Reverse Transcription kit (Applied Biosystem, Foster City, CA, USA) and Real-Time PCR was performed using the DyNamo SYBR Green qPCR kit (Thermo Fisher Scientific, Waltham, MA, USA). Genes primers sequences are listed in Table S2.

For Review Only

1
2
3
4
5
6
7
8
9
10
11
12
13
14
15
16
17
18
19
20
21
22
23
24
25
26
27
28
29
30
31
32
33
34
35
36
37
38
39
40
41
42
43
44
45
46
47
48
49
50
51
52
53
54
55
56
57
58
59
60

NanoString nCounter technology was performed by PharmaDiagen team (Pordenone, Italy) and the analysis was focused on 770 genes (nCounter PanCancer Progression Panel). Biological Process enrichment of significant modulated genes was identified through DAVID Functional Annotation Tools *(https://david.ncifcrf.gov)*. All Heatmaps were generated with Excel. Venny diagram was created by Venny 2.1 Tool (*http://bioinfogp.cnb.csic.es/tools/venny*) and pathway enrichment were generated with Panthers Classification System (http://pantherdb.org/).

Western blot analysis

Total proteins were extracted from cryopreserved melanoma biopsies and lysed in buffer pH 7.5. 10 μg of protein were separated on SDS-PAGE gels, transferred to nitrocellulose membranes (Bio-Rad Laboratories, Inc, Hercules, CA, USA), and incubated with primary antibodies (listed in Table S1) and then with peroxidase-conjugated anti-mouse or anti-rabbit secondary antibodies (Bio-Rad Laboratories). Proteins were visualized using Chemidoc MP Imager (Bio-Rad Laboratories) after incubation with ECL detection system (Pierce Biotechnology, Fisher Scientific International Inc., Hampton, NH, USA)

For Review Only

Melanoma skin reconstructs.

For dermal reconstructs, 0.5 ml of a cell free collagen solution (1.35 mg/ml rat tail type I collagen in DMEM with 10% FBS and 1% Pen/Strep) was added to tissue culture inserts (Transwell, Costar, Cambridge, MA) in 12-well plates. This pre-coated layer was overlaid with 1ml of fibroblasts mixed with collagen type I solution ($15x10^4$/ml). In case of DN melanoma, spheroids were implanted in the dermal equivalent and after 4 days of incubation at 37°C, primary human keratinocytes ($25x10^4$ cells) were seeded on it to form epidermal equivalent. As concern for CT melanoma, human keratinocytes and CT melanoma cells ($5x10^4$ cells) were seeded together on dermal reconstructs. Finally, skin reconstructs were exposed to the air and medium was changed every two days. After either 6 or 12

days, skin reconstructs were fixed with formalin for 2 h at room temperature, dehydrated and embedded in paraffin.

Statistical analysis

For clinical data, statistical analysis was performed using STATA® software version 14 (StataCorp. 2015. Stata Statistical Software: Release 14. StataCorp LP, College Station, TX, USA). Descriptive statistics were presented for baseline demographic clinical characteristics for the entire group. Means and standard deviations were calculated for normally distributed data while medians and 1st and 3rd quartiles were calculated for data that were not normally distributed. Continuous variables were presented as the number of patients (N), mean, standard deviation (SD), minimum (min), and maximum (max) and compared between subgroups using Unpaired Student's t test for two group; while categorical variables were presented as frequency (N, percentage [%]) and compared using Pearson's chi-squared test. A $p < 0.05$ was considered statistically significant.

For other data, the results are presented as mean ± SD from three independent experiments. Statistical analysis was performed with One-way ANOVA and Student's T-test by using GrapshPad Prism 9 (GraphPad software, La Jolla California, USA). Significant p-values are indicated with * for $p < 0.05$, ** for $p < 0.01$ and *** for $p < 0.001$.

For Review Only

1
2
3
4
5
6
7
8
9
10
11
12
13
14
15
16
17
18
19
20
21
22
23
24
25
26
27
28
29
30
31
32
33
34
35
36
37
38
39
40
41
42
43
44
45
46
47
48
49
50
51
52
53
54
55
56
57
58
59
60

Table S1: List of Primary antibody used in the study.

Antibody	Provider	Dilution	Application
HMB45	Ventana, Roche (Rotkreuz, Switzerland)	Ready to use	IHC
Melan-A	Ventana, Roche	Ready to use	IHC
$BRAF^{V600E}$	Ventana, Roche	Ready to use	IHC
Ki67	Dako, Agilent (Santa Clara, CA, USA)	1:200	IHC
MERTK	MilliporeSigma, (Burlington, MS, USA)	1:100	IHC
NESTIN	Arigo Biolaboratories (Hsinchu City, Taiwan)	1:100	IHC
HIF-1α	Novus Biologicals (Centennial, CO,USA)	1:50	IHC
ABCB5	Novus Biologicals	1:100	IHC
SOX-10	Novus Biologicals	1:200	IHC
SOX-2	Novus Biological	1:200	IHC/IF
CD133	Biorbyt (St Louis, MO, USA)	1:100	IHC
CD271	MilliporeSigma	1:100	IHC
E-CADHERIN	BD Bioscience (San Jose, CA, USA)	1:100 1:1000	IHC / IF WB
N-CADHERIN	BD Bioscience	1:100 1:1000	IHC / IF WB
α7 INTEGRIN	Santa Cruz Biotechnology (Dallas, TX, USA)	1:100 1:1000	IHC / IF WB
α4 INTEGRIN	Santa Cruz Biotechnology	1:100 1:1000	IHC / IF WB

For Review Only

1
2
3
4
5
6
7
8
9
10
11
12
13
14
15
16
17
18
19
20
21
22
23
24
25
26
27
28
29
30
31
32
33
34
35
36
37
38
39
40
41
42
43
44
45
46
47
48
49
50
51
52
53
54
55
56
57
58
59
60

Table S2: Primers for Real-Time PCR

	Forward primer	Reverse primer
βactin	TGG ATG ATG ATA TCG CCG CGC TCG	CAC ATA GGA ATC CTT CTG ACC CA
NGFR	TGA GTG CTG CAA AGC CTG CAA	TCT CAT CCT GGT AGT AGC CGT
BIRC5	GCA TGG GTG CCC CGA CGT TG	GCT CCG GCC AGA GGC CTC AA
CXCL8	GAATGGGTTTGCTAGAATGTGATA	CAGACTAGGGTTGCCAGATTTAAC

For Review Only

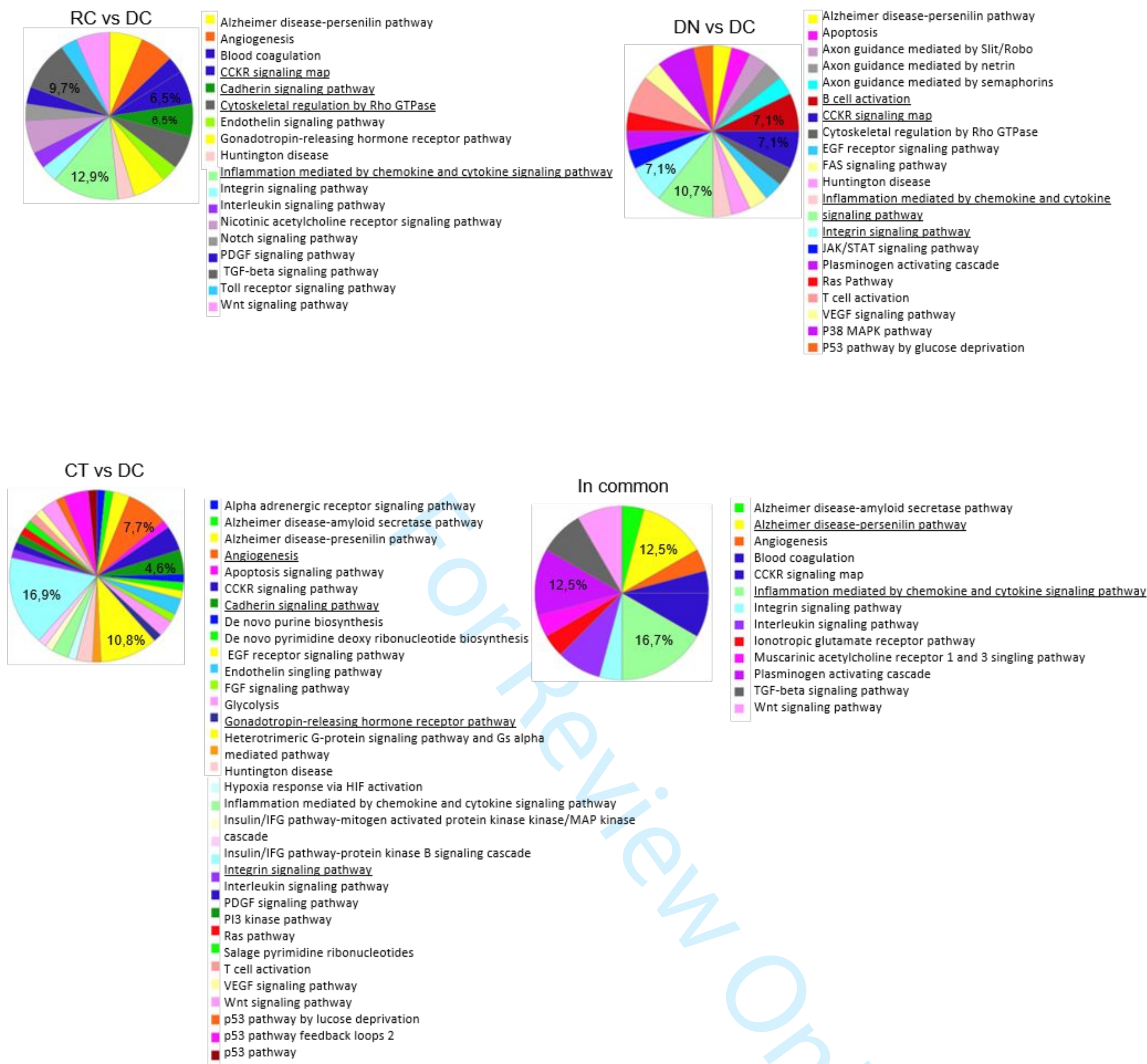

For Review Only

Figure S1. Panther pie chart of up-regulated gene in RCvsDC, CTvsDC and DNvsDC comparison. Differentially expressed genes within RCvsDC, CTvsDC and DNvsDC comparisons were analyzed by Venny 2.1 tool. Gene list from each comparison was subsequently uploaded on PANTHER Classification System to generate a "Pathway" pie chart. The percentage of gene hit against total Pathway hits was reported for the top five up-regulated pathways (underlined).

1
2
3
4
5
6
7
8
9
10
11
12
13
14
15
16
17
18
19
20
21
22
23
24
25
26
27
28
29
30
31
32
33
34
35
36
37
38
39
40
41
42
43
44
45
46
47
48
49
50
51
52
53
54
55
56
57
58
59
60

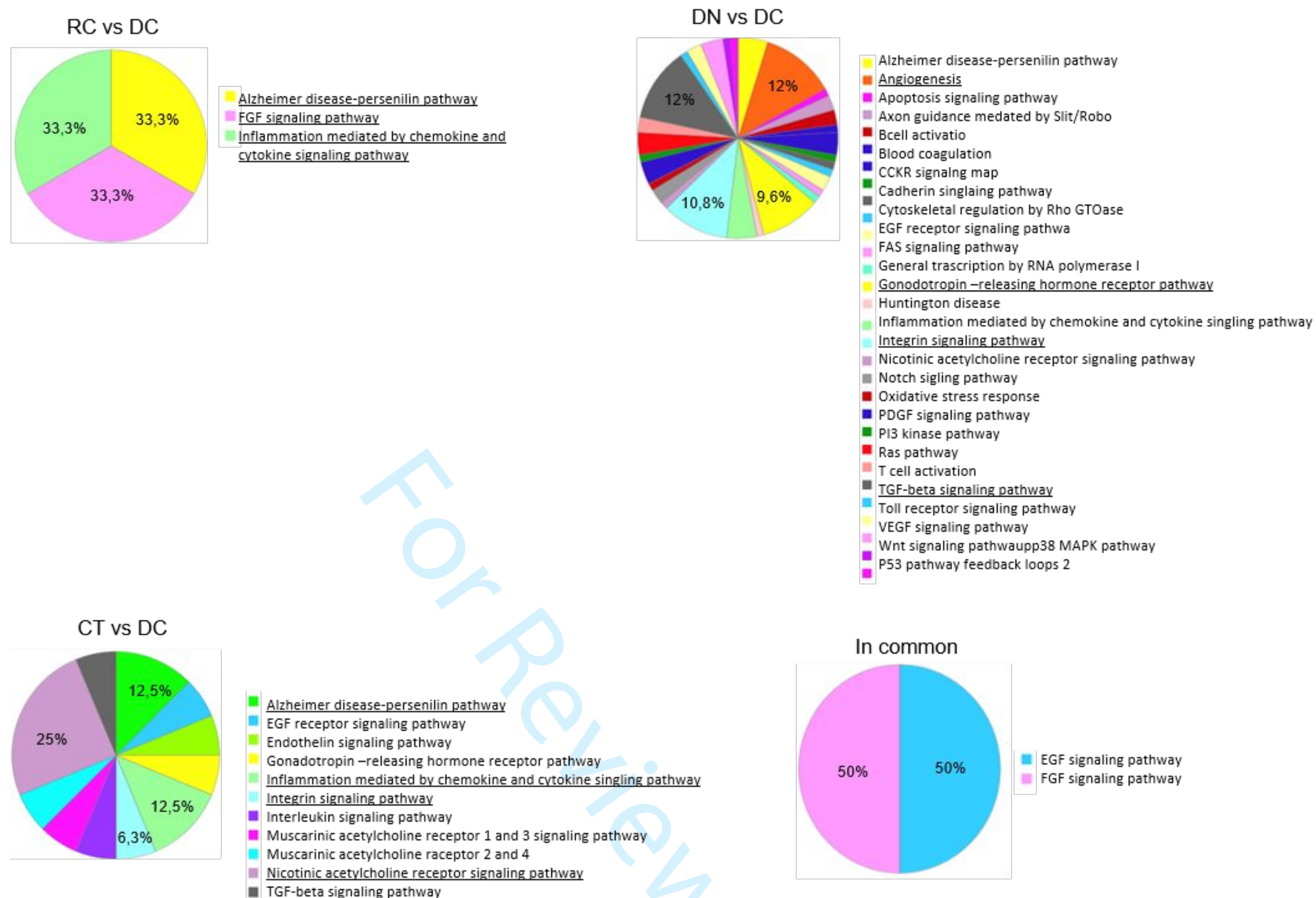

Figure S2. Panther pie chart of down-regulated gene in RCvsDC, CTvsDC and DNvsDC comparison. Differently expressed genes in RCvsDC, CTvsDC and DNvsDC comparison were uploaded onto Venny 2.1 tool. The gene list resulting modulated in each group obtained from Venny were uploaded on PANTHER Classification System to generate a pie chart related to involved pathways. Percent of gene hit against total Pathway hits were reported for the top five more up-regulated pathways (underlined).

For Review Only

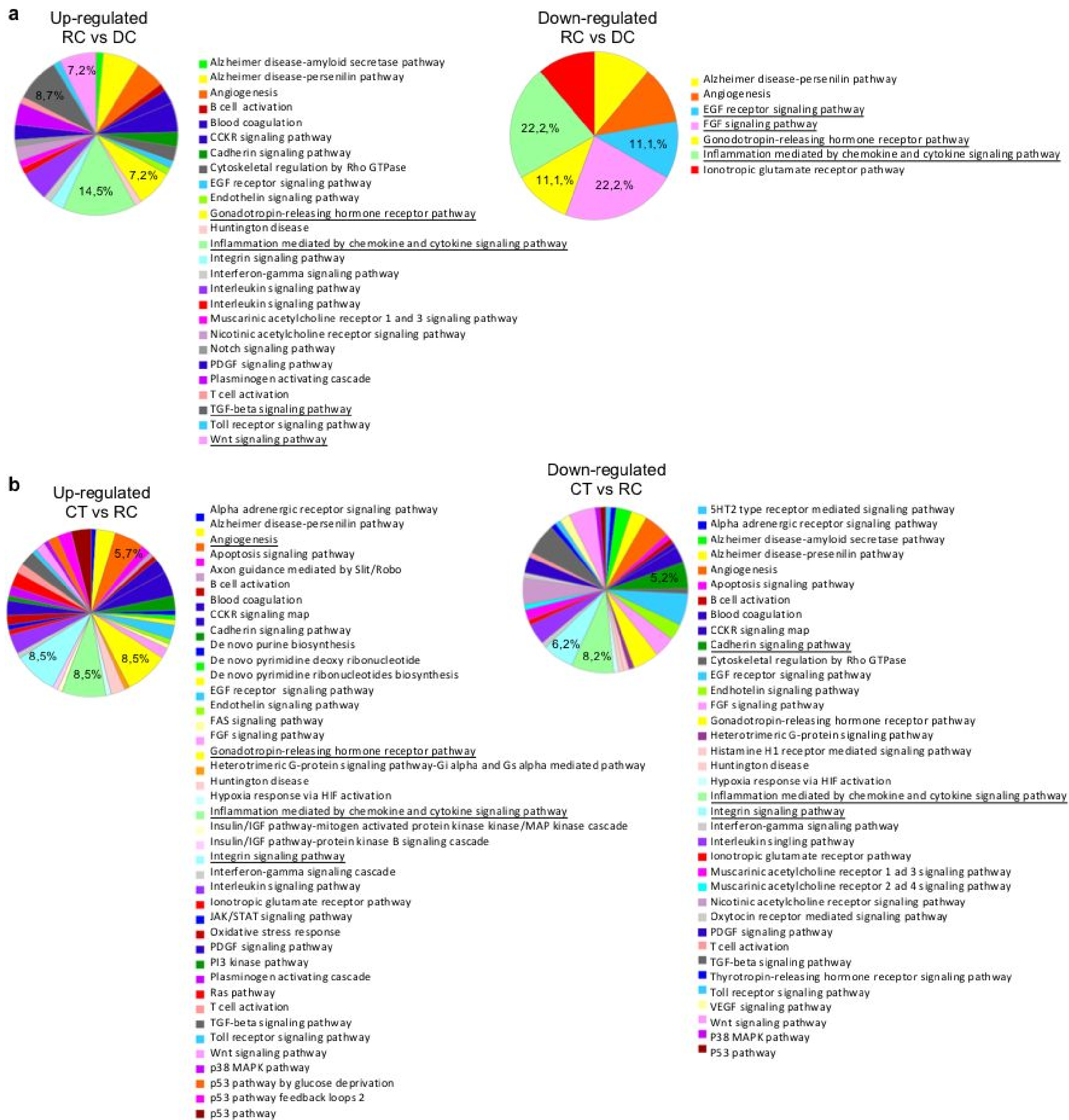

Figure S3. Panther pie chart of up and down-regulated gene in RC-DC and, CT-RC comparison. Differently expressed genes in (a) RCvsDC and (b) CTvsRC melanomas were uploaded on PANTHER Classification System to generate a pie chart related to involved pathways. Percent of gene hit against total Pathway hits were reported for the five more up-regulated pathways (underlined)

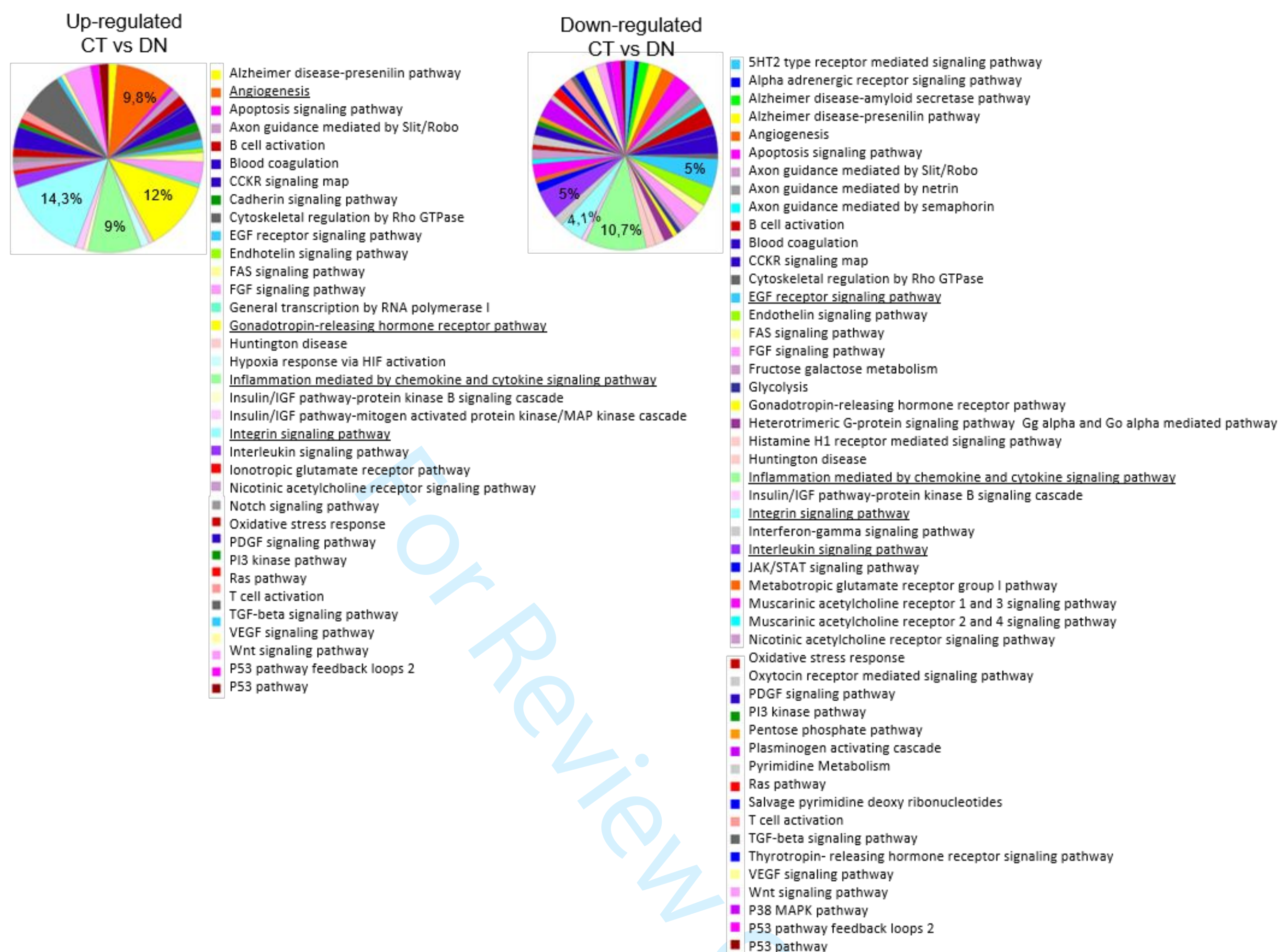

For Review Only

Figure S4. Panther pie chart of up and down-regulated gene in CT versus DN melanoma. Up-regulated and down-regulated genes in CT versus DN were uploaded on PANTHER Classification System to generate a pie chart related to involved pathways. Percent of gene hit against total Pathway hits were reported for the five more up-regulated pathways (underlined).

1
2
3
4
5
6
7
8
9
10
11
12
13
14
15
16
17
18
19
20
21
22
23
24
25
26
27
28
29
30
31
32
33
34
35
36
37
38
39
40
41
42
43
44
45
46
47
48
49
50
51
52
53
54
55
56
57
58
59
60

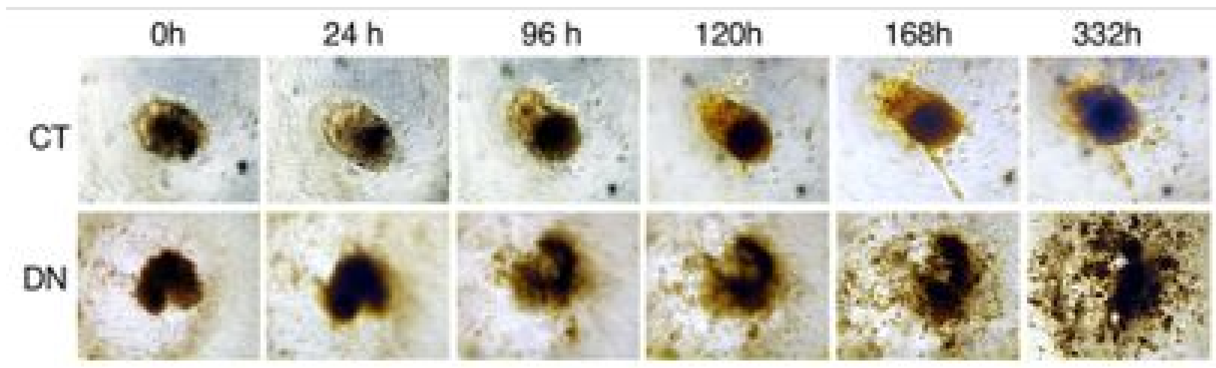

Figure S5. Collagen invasion assay of the most aggressive RCM-Subtypes. CT and DN melanoma biopsies were digested, and cells were seeded in hanging drop culture to obtain spheroids. 72 h after seeding, spheroids were transferred in a type I collagen matrix and pictures were taken from 0 to 332 hours.

For Review Only

1
2
3
4
5
6
7
8
9
10
11
12
13
14
15
16
17
18
19
20
21
22
23
24
25
26
27
28
29
30
31
32
33
34
35
36
37
38
39
40
41
42
43
44
45
46
47
48
49
50
51
52
53
54
55
56
57
58
59
60

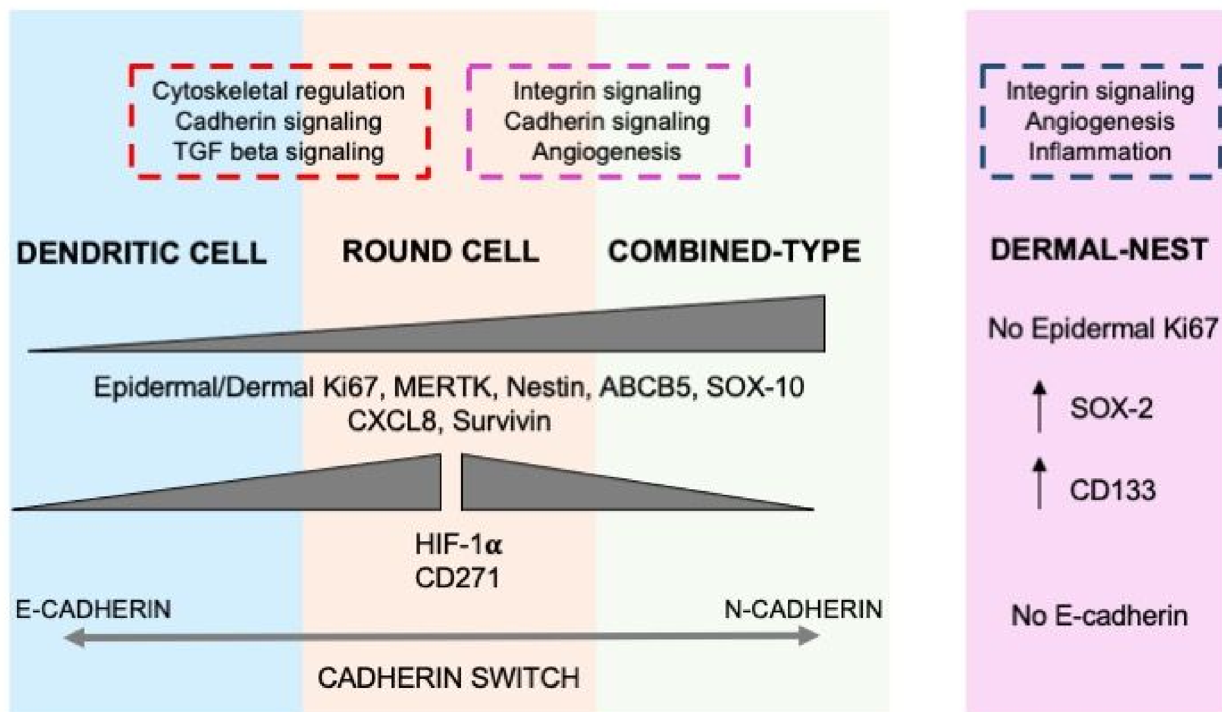

Figure S6. Schematic representation of the RCM-melanoma subtypes bio-molecular features and gene modulation.

view Only